Modelling and monitoring of INAR(1) process with geometrically inflated Poisson innovations

Cong Li[1,2], Haixiang Zhang[3*] and Dehui Wang[1]

[1] *Center for Applied Statistical Research, School of Mathematics, Jilin University, Changchun, 130012, China*

[2] *Key Laboratory for Applied Statistics of MOE, School of Mathematics and Statistics, Northeast Normal University, Changchun, 130024, China*

[3] *Center for Applied Mathematics, Tianjin University, Tianjin, 300072, China*

Abstract To analyse count time series data inflated at the $r+1$ values $\{0, 1, \cdots, r\}$, we propose a new first-order integer-valued autoregressive process with r-geometrically inflated Poisson innovations. Some statistical properties together with conditional maximum likelihood estimate are provided. For the purpose of statistical monitoring, we focus on the cumulative sum chart, exponentially weighted moving average chart and combined jumps chart towards the proposed process. Numerical simulations indicate that the conditional maximum likelihood estimator is unbiased. Moreover, the cumulative sum chart is the best choice to monitor our model in practice. Some applications about telephone complaints data are provided to illustrate the proposed methods.

Keywords: Combined jumps chart; Conditional maximum likelihood; CUSUM chart; EWMA chart; Integer-valued time series; Inflated distribution.

1 Introduction

Count time series data have attracted great interests of many researchers during the past years. Due to the special count structure, some traditional time series models fail to describe this kind of data. To solve this problem, Al-Osh and Alzaid (1987) proposed a novel first-order integer-valued autoregressive (INAR(1)) model based on the thinning operator "$\circ$" in Steutel and Van Harn (1979), which has laid the foundation of thinning-operator based methods in the field of integer-valued time series. Since then, a great number of related papers were published towards the topics on count time series data. To mention just a few examples, Zheng et al. (2007) proposed a first-order random coef-

*Corresponding author. Email: haixiang.zhang@tju.edu.cn (H. Zhang)

ficient integer-valued autoregressive process. Ristić et al. (2009) defined a new INAR(1) process with geometric distribution. Bakouch and Ristić (2010) proposed an INAR(1) process with zero truncated Poisson marginal distribution. Zhang et al. (2010; 2012) proposed some INAR processes with signed thinning operators. Schweer and Weiß (2014) considered a compound Poisson INAR(1) model for time series of overdispersed counts. Nastić et al. (2016) introduced a random environment in the integer-valued autoregressive process. Fernández-Fontelo et al. (2019) built an INAR(1) model for underreported counts. Lu (2019) studied the predictive distributions of count time series. Sellers et al. (2020) and Bourguignon et al. (2019) considered dispersed INAR(1) models. Jentsch and Weiß (2019) proposed a general INAR-type bootstrap procedure. Darolles et al. (2019) studied a new family of bivariate INAR models. For more literatures, we refer to the review papers by Weiß (2008) and Scotto et al. (2015).

From the view of practical application, count data may contain excess of certain values, so-called "inflated-values". One of the most common case is the zero-inflated data. For example, Jazi et al. (2012) introduced a new stationary first-order integer valued autoregressive process with zero inflated Poisson innovations. Li et al. (2015) proposed a first-order mixed integer-valued autoregressive process with zero-inflated generalized power series innovations. Barreto-Souza (2015), Bourguignon et al. (2018) and Bakouch et al. (2018) gave new zero-modified geometric INAR processes for count time series with deflation or inflation of zeros respectively. Möller et al. (2018) and Kang et al. (2019) developed zero pattern INAR models with bounded supports respectively. Shamma et al. (2020) and Möller et al. (2020) also proposed state-dependent zero inflation INAR(1) models. Weiß et al. (2019) developed several tests for zero inflation in INAR(1) models. However, the real count data may inflated at several values instead of a single inflated value at zero (Rakitzis et al., 2016; 2018).

Statistical quality control (SQC) is often concerned with count data (Xie et al., 2001). The monitoring of INAR(1) processes has received sustaining attention in the literature. For instance, Weiß and Testik (2009; 2011), Weiß (2009a, 2009b, 2011), Yontay et al. (2013), Zhang et al. (2014), Sales et al. (2020), Cabral Morais and Knoth (2020) all developed some strategies to monitor Poisson INAR(1) processes respectively. Li et al. (2019a) proposed some effective control charts for monitoring the zero truncated INAR(1) processes respectively. Rakitzis et al. (2017), Kim and Lee (2019) studied

the controlling methods of zero-inflated Poisson INAR(1) models respectively. Li et al. (2019b) explored the monitoring of zero-inflated geometric INAR(1) processes. Vanli et al. (2019) presented control charts for Poisson integer valued GARCH models. Li et al. (2020) considered INAR control charts for simultaneously detecting shifts in both the marginal mean and the autocorrelation coefficient. In this work, we propose a novel first-order integer-valued autoregressive process with geometrically inflated Poisson innovations (INAR-GIP(1)), which is more flexible in practical application. Our model can fit count time series data inflated at the $r+1$ values $\{0, 1, \cdots, r\}$, and Jazi et al. (2012) can be viewed as a special case of our proposed INAR-GIP(1) process. Moreover, we monitor the INAR-GIP(1) process by the cumulative sum (CUSUM) control chart, exponentially weighted moving average (EWMA) control chart and combined jumps control chart, respectively.

The remainder of the paper is organized as follows. In Section 2, we propose a new INAR(1) process with geometrically inflated Poisson innovations. Some statistical properties of the process, together with the estimation method of parameters are provided. In Section 3, the CUSUM, EWMA and combined jumps charts for the INAR-GIP(1) process are studied. Section 4 presents some simulation results. In Section 5, we apply our proposed methods to two real data examples. Some concluding remarks are given in Section 6.

2 The INAR-GIP(1) process

In this section, we propose a new INAR-GIP(1) process to handle the non-negative integer-valued time series data with inflated values at $\{0, 1, \cdots, r\}$. Some basic statistical properties of the INAR-GIP(1) process are established. We use the conditional maximum likelihood (CML) method to estimate the unknown parameters in the INAR-GIP(1) process.

2.1 Construction and some properties of the process

First we review the r-geometrically inflated Poisson distribution, which was proposed by Rakitzis et al. (2016). A random variable ε_t is said to follow the geometrically inflated Poisson distribution of order r with parameters ϕ and λ (denoted as $\text{GIP}_r(\phi, \lambda)$), if its

probability mass function is given as

$$P(\varepsilon_t = k) = \begin{cases} \frac{1}{r+1}\phi^{k+1} + \left(1 - \frac{1}{r+1}\sum_{i=0}^{r}\phi^{i+1}\right)\frac{\lambda^k e^{-\lambda}}{k!}, & \text{if } k \in \{0, \cdots, r\}, \\ \left(1 - \frac{1}{r+1}\sum_{i=0}^{r}\phi^{i+1}\right)\frac{\lambda^k e^{-\lambda}}{k!}, & \text{if } k \in \{r+1, \cdots\}, \end{cases}$$

where $\phi \in [0,1]$, $\lambda > 0$ and $r \in \mathbb{N}$. As pointed out by Rakitzis et al. (2016), the $\text{GIP}_r(\phi, \lambda)$ distribution is inflated at the first $r+1$ values $\{0, 1, \cdots, r\}$. Of note, the $\text{GIP}_r(\phi, \lambda)$ distribution reduces to zero-inflated Poisson distribution with parameters ϕ and λ if $r = 0$; and it reduces to Poisson distribution with parameter λ when $\phi = 0$.

For simplicity, we denote $g(r, \phi) = 1 - \frac{1}{r+1}\sum_{i=0}^{r}\phi^{i+1}$ in the following context. By Rakitzis et al. (2016), the probability generating function of $\text{GIP}_r(\phi, \lambda)$ distribution is

$$\Phi_{\text{GIP}_r}(s) = \frac{1}{r+1}\sum_{i=0}^{r} s^i \phi^{i+1} + g(r, \phi)e^{\lambda(s-1)}. \tag{2.1}$$

If ε_t follows from $\text{GIP}_r(\phi, \lambda)$, the mean, variance and kth order moments of ε_t are $\mu_\varepsilon = \text{E}(\varepsilon_t) = \frac{1}{r+1}\sum_{i=1}^{r} i\phi^{i+1} + g(r, \phi)\lambda$, $\sigma_\varepsilon^2 = \text{Var}(\varepsilon_t) = \frac{1}{r+1}\sum_{i=1}^{r} i^2\phi^{i+1} + g(r, \phi)\lambda(1+\lambda) - \mu_\varepsilon^2$, and $\text{E}(\varepsilon_t^k) = \frac{1}{r+1}\sum_{i=1}^{r} i^k\phi^{i+1} + g(r, \phi)\text{E}(W^k)$, where $W \sim \text{Poisson}(\lambda)$. Here we point out that the $\sigma_\varepsilon^2/\mu_\varepsilon$ may be equal to 1, greater than 1, or less than 1 (Rakitzis et al., 2016). Thus, the GIP_r distribution could fit a broad class of data with various levels of dispersion.

To construct the INAR-GIP(1) process, we employ the binomial thinning operator " $\circ$ " (Steutel and Van Harn, 1979) defined as $\alpha \circ X = \sum_{i=1}^{X} Y_i$, where $\{Y_i\}$ is a sequence of independent and identically distributed (i.i.d.) Bernoulli random variables with $P(Y_i = 1) = 1 - P(Y_i = 0) = \alpha$. Below, we give some details about the proposed INAR-GIP(1) process.

Definition 1. *The INAR-GIP(1) process $\{X_t\}$ is defined by the following recursive equation:*

$$X_t = \alpha \circ X_{t-1} + \varepsilon_t, \quad t = 0, 1, 2, \cdots, \tag{2.2}$$

where $\alpha \circ X_{t-1} = \sum_{i=1}^{X_{t-1}} Y_{it}$ with $\alpha \in (0,1)$, the $\{\varepsilon_t\}$ is a sequence of i.i.d. $GIP_r(\phi, \lambda)$ random variables; ε_t is independent of all Bernoulli count series $\{Y_{it}\}$. Let $\mu_\varepsilon = \text{E}(\varepsilon_t)$ and $\sigma_\varepsilon^2 = \text{Var}(\varepsilon_t)$, which are assumed to be finite. The sequence of $\{\varepsilon_t\}$ is called the innovation series and the INAR-GIP(1) process is an INAR(1) process with r-geometrically inflated Poisson innovations.

Obviously, when $\phi = 0$ the INAR-GIP(1) process is reduced to Poisson INAR(1) process (Al-Osh and Alzaid, 1987); and when $r = 0$ and $\phi > 0$, the INAR-GIP(1) process is reduced to ZIPINAR(1) process (Jazi et al., 2012). The proposed INAR-GIP(1) process could be viewed as a Markov process or a Galton-Waston branching process with immigration. From the view of branching process, the $\alpha \circ X_{t-1}$ can be interpreted as the number of offspring at time t from the previous period $t-1$, where α can be interpreted as the survival probability of an individual offspring, and ε_t is the number of new immigrants at time t. Based on the branching process theorem in Heathcote (1966), if we impose two conditions $0 < \alpha < 1$ and $\frac{1}{r+1}\sum_{i=1}^{r} i\phi^{i+1} + g(r,\phi)\lambda < \infty$ on our model (2.2), the resulting INAR-GIP(1) process is strictly stationary, irreducible and aperiodic. In the remainder of this article, we assume $\{X_t\}$ satisfies the above two conditions. Now we give some moments and conditional moments of the INAR-GIP(1) process.

Theorem 1. *Let $\{X_t\}$ be the INAR-GIP(1) process given in (2.2), then*

(i). $\mu_X = \mathrm{E}(X_t) = \dfrac{\mu_\varepsilon}{1-\alpha}$;

(ii). $\sigma_X^2 = \mathrm{Var}(X_t) = \dfrac{\alpha\mu_\varepsilon + \sigma_\varepsilon^2}{1-\alpha^2}$;

(iii). $\mathrm{E}(X_{t+k}|X_t) = \alpha^k X_t + \dfrac{1-\alpha^k}{1-\alpha}\mu_\varepsilon, \quad k = 1, 2, \cdots$;

(iv). $\mathrm{Var}(X_{t+k}|X_t) = \alpha^k(1-\alpha^k)(X_t - \mu_X) + (1-\alpha^{2k})\sigma_X^2, \quad k = 1, 2, \cdots$;

(v). $\mathrm{Corr}(X_{t+k}, X_t) = \alpha^k, \quad k = 1, 2, \cdots$.

Proof. (i). Note that

$$\mathrm{E}(X_t) = \mathrm{E}(\alpha \circ X_{t-1} + \varepsilon_t) = \alpha\mathrm{E}(X_{t-1}) + \mu_\varepsilon.$$

Since $\{X_t\}$ is a strictly stationary process, we have $\mu_X \equiv \mathrm{E}(X_t) = \frac{\mu_\varepsilon}{1-\alpha}$.

(ii). Due to $X_t = \alpha \circ X_{t-1} + \varepsilon_t$, we can derive that

$$\begin{aligned}
\mathrm{E}(X_t^2) &= \mathrm{E}[(\alpha \circ X_{t-1} + \varepsilon_t)^2] \\
&= \mathrm{E}[(\alpha \circ X_{t-1})^2] + \mathrm{E}(\varepsilon_t^2) + 2\mathrm{E}[(\alpha \circ X_{t-1})\varepsilon_t] \\
&= \alpha^2\mathrm{E}(X_{t-1}^2) + \alpha(1-\alpha)\mathrm{E}(X_{t-1}) + \mathrm{Var}(\varepsilon_t) + \mathrm{E}^2(\varepsilon_t) + 2\alpha\mathrm{E}(X_t)\mathrm{E}(\varepsilon_t) \\
&= \alpha^2\mathrm{E}(X_{t-1}^2) + \alpha\mu_\varepsilon + \sigma_\varepsilon^2 + \mu_\varepsilon^2 + \frac{2\alpha\mu_\varepsilon^2}{1-\alpha}.
\end{aligned}$$

By the stationarity of the process, we know

$$\mathrm{E}(X_t^2) = \frac{\alpha(1-\alpha)\mu_\varepsilon + (1-\alpha)\sigma_\varepsilon^2 + (1+\alpha)\mu_\varepsilon^2}{(1-\alpha)^2(1+\alpha)}.$$

Then,

$$\mathrm{Var}(X_t) = \mathrm{E}(X_t^2) - \mu_X^2 = \frac{\alpha\mu_\varepsilon + \sigma_\varepsilon^2}{1-\alpha^2}.$$

(iii). The one-step conditional mean is

$$\mathrm{E}(X_{t+1}|X_t) = \mathrm{E}(\alpha \circ X_t + \varepsilon_{t+1}|X_t) = \alpha X_t + \mu_\varepsilon. \tag{2.3}$$

By repeated application of (2.3), it is easy to obtain that

$$\mathrm{E}(X_{t+k}|X_t) = \alpha^k X_t + \frac{1-\alpha^k}{1-\alpha}\mu_\varepsilon.$$

(iv). Furthermore,

$$\begin{aligned}
\mathrm{E}(X_{t+1}^2|X_t) &= \mathrm{E}((\alpha \circ X_t + \varepsilon_{t+1})^2|X_t) \\
&= \alpha^2 X_t^2 + \alpha(1-\alpha)X_t + \mathrm{E}(\varepsilon_{t+1}^2) + 2\alpha\mu_\varepsilon X_t \\
&= \alpha^2 X_t^2 + [\alpha(1-\alpha) + 2\alpha\mu_\varepsilon]X_t + \mathrm{E}(\varepsilon_{t+1}^2).
\end{aligned}$$

By the proof of (ii), we have $\mathrm{E}(\varepsilon_t^2) = (1-\alpha^2)\mathrm{E}(X_t^2) - [\alpha(1-\alpha) + 2\alpha\mu_\varepsilon]\mathrm{E}(X_t)$. Then

$$\mathrm{E}(X_{t+1}^2|X_t) = \alpha^2 X_t^2 + [\alpha(1-\alpha) + 2\alpha\mu_\varepsilon](X_t - \mathrm{E}(X_t)) + (1-\alpha^2)\mathrm{E}(X_t^2).$$

Then using the induction method, we obtain

$$\mathrm{E}(X_{t+k}^2|X_t) = \alpha^{2k} X_t^2 + \frac{[\alpha(1-\alpha) + 2\alpha\mu_\varepsilon]\alpha^k(1-\alpha^k)}{\alpha(1-\alpha)}(X_t - \mathrm{E}(X_t)) + (1-\alpha^{2k})\mathrm{E}(X_t^2).$$

Also the k-ahead conditional variance takes the following form,

$$\begin{aligned}
\mathrm{Var}(X_{t+k}|X_t) &= \mathrm{E}(X_{t+k}^2|X_t) - \mathrm{E}(X_{t+k}|X_t)^2 \\
&= \alpha^k(1-\alpha^k)(X_t - \mathrm{E}(X_t)) + (1-\alpha^{2k})(\mathrm{E}(X_t^2) - \mathrm{E}(X_t)^2) \\
&= \alpha^k(1-\alpha^k)(X_t - \mu_X) + (1-\alpha^{2k})\sigma_X^2.
\end{aligned}$$

(v). Since

$$\mathrm{E}(X_{t+k}X_t) = \mathrm{E}[\mathrm{E}(X_{t+k}X_t|X_t)] = \mathrm{E}[X_t\mathrm{E}(X_{t+k}|X_t)]$$

$$
\begin{aligned}
&= \mathrm{E}\left[X_t\left(\alpha^k X_t + \frac{1-\alpha^k}{1-\alpha}\mu_\varepsilon\right)\right] \\
&= \alpha^k \mathrm{E}(X_t^2) + \frac{1-\alpha^k}{1-\alpha}\mu_\varepsilon \mathrm{E}(X_t).
\end{aligned}
$$

Thus, we know that $\mathrm{Corr}(X_{t+k}, X_t) = \alpha^k$. This completes the proof. □

From the above theorem, we can see that $\lim_{k\to\infty} \mathrm{E}(X_{t+k}|X_t) = \mu_\varepsilon/(1-\alpha) = \mathrm{E}(X_t)$, which is the unconditional mean of the process, $\lim_{k\to\infty} \mathrm{Var}(X_{t+k}|X_t) = \mathrm{Var}(X_t)$, which is the unconditional variance of the process. According to Theorem 1, we can also get the variance-to-mean ratio of the INAR-GIP(1) process $\{X_t\}$

$$
\frac{\sigma_X^2}{\mu_X} = \frac{\alpha\mu_\varepsilon + \sigma_\varepsilon^2}{\alpha\mu_\varepsilon + \mu_\varepsilon}.
$$

So the $\{X_t\}$ is overdispersed for $\sigma_\varepsilon^2/\mu_\varepsilon > 1$, or underdispersed for $\sigma_\varepsilon^2/\mu_\varepsilon < 1$, or equidispersed for $\sigma_\varepsilon^2/\mu_\varepsilon = 1$. From this point of view, our proposed INAR-GIP(1) process is very flexible, which can describe an extensive kinds of count time series data for practical application.

The transition probability of $\{X_t\}$ plays an important role in the likelihood-based estimation methods, it is straight-forward to derive that

$$
p_{ij} = P(X_t = j|X_{t-1} = i) = \sum_{k=0}^{min\{i,\ j\}} P(\varepsilon_t = j-k)\binom{i}{k}\alpha^k(1-\alpha)^{i-k}, \quad i,\ j = 0,\ 1, \cdots .
$$

Moreover, the marginal distribution of INAR-GIP(1) process could be expressed in terms of the innovation sequence $\{\varepsilon_t\}$ with $X_t = \sum_{j=0}^{\infty} \alpha^j \circ \varepsilon_{t-j}$ (Al-Osh and Alzaid, 1987). Then we can get the probability generating function of $\{X_t\}$

$$
\Phi_{X_t}(s) = \prod_{j=0}^{\infty}\left[\frac{1}{r+1}\sum_{i=0}^{r}(1+\alpha^j s - \alpha^j)^i \phi^{i+1} + g(r,\phi)e^{-\lambda\alpha^j(1-s)}\right]. \tag{2.4}
$$

Based on (2.4), the corresponding probability mass function of $\{X_t\}$ is given as

$$
P(X_t = k) = \Phi_X^{(k)}(0)/k!, \text{ for } k = 0, 1, \cdots , \tag{2.5}
$$

where $\Phi_X^{(k)}(s)$ denotes the kth derivative of $\Phi_X(s)$. More specifically, we present the probability mass function of $\{X_t\}$ at "0" and "1", where

$$
P(X_t = 0) = \prod_{j=0}^{\infty}\left[\frac{1}{r+1}\sum_{i=0}^{r}(1-\alpha^j)^i \phi^{i+1} + g(r,\phi)e^{-\lambda\alpha^j}\right]
$$

and

$$P(X_t=1)=\sum_{k=0}^{\infty}\left[\left(\frac{1}{r+1}\alpha^k\sum_{i=1}^{r}i(1-\alpha^k)^{i-1}\phi^{i+1}+g(r,\phi)\lambda\alpha^k e^{-\lambda\alpha^k}\right)\right.$$
$$\left.\times\prod_{j\neq k}\left(\frac{1}{r+1}\sum_{i=0}^{r}(1-\alpha^j)^i\phi^{i+1}+g(r,\phi)e^{-\lambda\alpha^j}\right)\right].$$

In the following theorem, we also give k-step ahead forecasting distribution of our proposed INAR-GIP(1) process.

Theorem 2. *The conditional probability generating function of X_{t+k} given X_t is given by*

$$\Phi_{X_{t+k}|X_t}(s)=(1+s\alpha^k-\alpha^k)^{X_t}\prod_{j=0}^{k-1}\left[\frac{1}{r+1}\sum_{i=0}^{r}(1+s\alpha^j-\alpha^j)^i\phi^{i+1}+g(r,\phi)e^{-\lambda\alpha^j(1-s)}\right],$$
$$k=1,2,\cdots.$$

Proof. Note that

$$\begin{aligned}X_{t+k}=&\alpha\circ X_{t+k-1}+\varepsilon_{t+k}=\alpha\circ(\alpha\circ X_{t+k-2}+\varepsilon_{t+k-1})+\varepsilon_{t+k}\\=&\cdots\\=&\alpha^k\circ X_t+\sum_{j=1}^{k}\alpha^{k-j}\circ\varepsilon_{t+j}=\alpha^k\circ X_t+\sum_{j=0}^{k-1}\alpha^j\circ\varepsilon_{t+k-j}.\end{aligned}$$

Then we have

$$\begin{aligned}\Phi_{X_{t+k}|X_t}(s)=&\mathrm{E}(s^{X_{t+k}}|X_t)\\=&\mathrm{E}(s^{\alpha^k\circ X_t+\sum_{j=0}^{k-1}\alpha^j\circ\varepsilon_{t+k-j}}|X_t)\\=&\mathrm{E}(s^{\alpha^k\circ X_t}|X_t)\mathrm{E}(s^{\sum_{j=0}^{k-1}\alpha^j\circ\varepsilon_{t+k-j}})\\=&\mathrm{E}(s^{\alpha^k\circ X_t}|X_t)\prod_{j=0}^{k-1}\mathrm{E}(s^{\alpha^j\circ\varepsilon_{t+k-j}}).\end{aligned}$$

Since $\alpha^k\circ X_t|X_t\sim B(X_t,\alpha^k)$, $\mathrm{E}(s^{\alpha^k\circ X_t}|X_t)=(1+s\alpha^k-\alpha^k)^{X_t}$ and

$$\begin{aligned}\prod_{j=0}^{k-1}\mathrm{E}(s^{\alpha^j\circ\varepsilon_{t+k-j}})=&\prod_{j=0}^{k-1}\mathrm{E}(s^{\alpha^j\circ\varepsilon_t})=\prod_{j=0}^{k-1}\mathrm{E}_{\varepsilon_t}[\mathrm{E}(s^{\alpha^j\circ\varepsilon_t}|\varepsilon_t)]\\=&\prod_{j=0}^{k-1}\mathrm{E}(1+s\alpha^j-\alpha^j)^{\varepsilon_t}\\=&\prod_{j=0}^{k-1}\left[\frac{1}{r+1}\sum_{i=0}^{r}(1+s\alpha^j-\alpha^j)^i\phi^{i+1}+g(r,\phi)e^{-\lambda\alpha^j(1-s)}\right].\end{aligned}$$

Hence, the result.

This completes the proof. □

As $k \to \infty$, the k-step ahead conditional probability generating function $\Phi_{X_{t+k}|X_t}(s)$ converges to the marginal probability generating function of the process $\{X_t\}$, that is, $\lim_{k\to\infty} \Phi_{X_{t+k}|X_t}(s) = \Phi_{X_t}(s)$. Since the probability generating function uniquely determines the probability mass function, the k-step ahead forecasting distribution of X_{t+k} given X_t converges to the marginal distribution of X_t.

The sequence of jumps $\{J_t\}_N$ is an interesting feature of the correlated process, which is defined by $J_t = X_t - X_{t-1}$, $t \geqslant 1$. Now we present some properties of the statistic J_t in a stationary INAR-GIP(1) process.

Theorem 3. *Let $\{X_t\}_{N_0}$ be a stationary INAR-GIP(1) process, then the moment generating function of J_t is given by*

$$M_{J_t}(s) = \left[\frac{1}{r+1}\sum_{i=0}^{r} e^{si}\phi^{i+1} + g(r,\phi)e^{\lambda(e^s-1)}\right] * \left\{\prod_{j=0}^{\infty}\frac{1}{r+1}\sum_{i=0}^{r}\left[1-\alpha^j(1-\alpha)(1-e^{-s})\right]^i\phi^{i+1} + g(r,\phi)e^{-\lambda\alpha^j(1-\alpha)(1-e^{-s})}\right\}. \tag{2.6}$$

Proof. Let $\Phi_{X_t,X_{t-1}}(s_0,s_1)$ be the probability generating functions of the bivariate random variable (X_t, X_{t-1}). We have that

$$\begin{aligned}
&\Phi_{X_t,X_{t-1}}(s_0,s_1) = E[s_0^{X_t}s_1^{X_{t-1}}] = E[s_0^{\alpha\circ X_{t-1}+\varepsilon_t}s_1^{X_{t-1}}] = E[s_0^{\varepsilon_t}s_1^{X_{t-1}}E(s_0^{\alpha\circ X_{t-1}}|X_{t-1})]\\
=&\Phi_{\varepsilon_t}(s_0)E\left[s_1^{X_{t-1}}(1+s_0\alpha-\alpha)^{X_{t-1}}\right] = \Phi_{\varepsilon_t}(s_0)\Phi_{X_t}\left(s_1(1+s_0\alpha-\alpha)\right)\\
=&\left[\frac{1}{r+1}\sum_{i=0}^{r}s_0^i\phi^{i+1} + g(r,\phi)e^{\lambda(s_0-1)}\right] * \left\{\prod_{j=0}^{\infty}\frac{1}{r+1}\sum_{i=0}^{r}\left[1+\alpha^j s_1(1+s_0\alpha-\alpha)-\alpha^j\right]^i\phi^{i+1}\right.\\
&\left. + g(r,\phi)e^{-\lambda\alpha^j[1-s_1(1+s_0\alpha-\alpha)]}\right\}.
\end{aligned}$$

Let $M_{J_t}(s)$ be the moment generating function of the random variable J_t, then we have

$$\begin{aligned}
M_{J_t}(s) =&E[\mathrm{e}^{sJ_t}] = E[\mathrm{e}^{sX_t}\mathrm{e}^{-sX_{t-1}}] = \Phi_{X_t,X_{t-1}}(\mathrm{e}^s,\mathrm{e}^{-s})\\
=&\left[\frac{1}{r+1}\sum_{i=0}^{r}e^{si}\phi^{i+1} + g(r,\phi)e^{\lambda(e^s-1)}\right] * \left\{\prod_{j=0}^{\infty}\frac{1}{r+1}\sum_{i=0}^{r}\left[1-\alpha^j(1-\alpha)(1-e^{-s})\right]^i\phi^{i+1}\right.\\
&\left. + g(r,\phi)e^{-\lambda\alpha^j(1-\alpha)(1-e^{-s})}\right\}.
\end{aligned}$$

This completes the proof. □

It's also easy to obtain $E(J_t) = 0$, $\mathrm{Var}(J_t) = 2(\alpha\mu_\varepsilon + \sigma_\varepsilon^2)/(1+\alpha)$, and the autocorrelation $\rho_J(k) = \alpha^{k-1}(\alpha-1)/2$. In Section 3 below, we shall introduce a combined jumps chart, which monitors the counts and jumps in the INAR-GIP(1) process simultaneously.

2.2 Estimation of parameters in the INAR-GIP(1) process

For the INAR-GIP(1) model, the number of unknown parameters does not change if the r varies. As suggested by Rakitzis et al. (2016), the r can be regarded as a nuisance parameter. In practice, we can use the AIC or BIC criterion to choose the best r for analysis. We are interested in estimating the parameters α, ϕ and λ. Given r and $\{x_1, \cdots, x_n\}$, the likelihood function for model (2.2) is given as

$$\begin{aligned} L_0 =& P(X_1 = x_1, X_2 = x_2, \cdots, X_n = x_n) \\ =& P(X_1 = x_1)P(X_2 = x_2|X_1 = x_1)\cdots P(X_n = x_n|X_{n-1} = x_{n-1}) \\ =& P(X_1 = x_1)\prod_{t=2}^{n}\left[\sum_{k=0}^{min\{x_{t-1},\ x_t\}} P(\varepsilon_t = x_t - k)\binom{x_{t-1}}{k}\alpha^k(1-\alpha)^{x_{t-1}-k}\right]. \end{aligned}$$

However, the expression of marginal probability function $P(X_1 = x_1)$ is very complicated in (2.5). Similar to Li et al. (2015), we can estimate the parameters of interest by maximizing the conditional maximum likelihood (CML) function

$$L = \prod_{t=2}^{n}\left[\sum_{k=0}^{min\{x_{t-1},\ x_t\}} P(\varepsilon_t = x_t - k)\binom{x_{t-1}}{k}\alpha^k(1-\alpha)^{x_{t-1}-k}\right]. \tag{2.7}$$

Existing Matlab function "fmincon" can be directly used to carry out the procedure.

3 Control charts for monitoring the process mean

In this section, we will study effective control charts for monitoring the INAR-GIP(1) process. As INAR(1) processes are always implemented as the numbers of jobless, defective goods and infectious patients, the upward shifts in the process mean stand for the increasing of the unemployment rate and the defective percentage, the spread of the disease. They are usually crucial and shall be identified and reported in time. Therefore for practical application considerations, the mean upward shift of the INAR-GIP(1) process is studied in this paper.

There are several papers in literature on monitoring procedures for INAR(1) processes, which fall into two main categories, the single control chart and the mixed control chart. In this paper, we investigate the effectiveness of three representative control charts, including two single control chart (the CUSUM chart and the EWMA chart) and one mixed control chart (the combined jumps chart).

The CUSUM chart is the first method we use, which was firstly proposed by Page (1961). The theory of the CUSUM chart is based on sequential probability ratio test, the idea is to accumulate the sample data information and accumulate the small deviation of the process to enlarge the effect. The CUSUM chart has proved to be effective to monitor integer-valued time series, such as Poisson INAR(1) (Weiß and Testik, 2009; 2011), NGINAR(1) (Li el al., 2016), ZIPINAR(1) and INARCH(1) (Rakitzis et al., 2017), etc. The CUSUM chart is also applied in this paper to the geometrically inflated count time series. We start with $C_0 = c_0$, $c_0 \in N_0$, a CUSUM statistic with reference value w is obtained by $C_t = \max(0,\ X_t - w + C_{t-1}),\ t = 1,\ 2, \cdots$. Then we have the following results.

Scheme 1 *(The CUSUM chart). Denote w, UCL$\in N$ with $\mu_X \leq w < UCL$, the monitoring statistics $\{C_t\}_{N_0}$ are plotted on a CUSUM chart with control region* $[0,\ UCL]$. *The INAR-GIP(1) process is considered as being in control unless $C_t > UCL$.*

The process is considered to be out-of-control when the CUSUM statistic C_t exceeds control limit UCL. Further investigation should be done on the basis of specific circumstances. The values of chart designs (w, UCL) are decided by the procedure to assess the performance of the chart. Average run length (ARL), the expected value of the number of sampling points until the chart signalizes an alarm, is the most common measure to assess the performance of the control chart. For an efficient control chart, a large in-control ARL (denoted as ARL_0) together with small out-of-control ARLs is necessary. The values of (w, UCL) are determined such that the in-control ARL (ARL_0) can be close to a given value, e.g. $\text{ARL}_0 = 370$. Now it comes to compute the values of ARL basing on the model parameters and CUSUM chart designs. As $\{X_t\ , C_t\}_{N_0}$ of the INAR-GIP(1) process forms a bivariate Markov chain, the Markov chain approach introduced in Weiß and Testik (2009) could also be used here for computing ARL. To give a complete picture of the computing method, we briefly explain this technique in the following.

For the CUSUM chart, the set of reachable in-control values of the bivariate Markov process $\{X_t, C_t\}_{N_0}$ is given by

$$\begin{aligned}\mathcal{CR}_1 &\triangleq \{(n,i) \in N_0 \times \{0,\cdots,UCL\} | \max(0, n-w+i) \in \{0,\cdots,UCL\}\} \\ &= \{(n,i) | 0 \leqslant i \leqslant UCL, \max(0, i+w-UCL) \leqslant n \leqslant i+w\},\end{aligned}$$

which is finite and could be ordered in a certain manner. The transition probability matrix of $\{X_t, C_t\}_{N_0}$ is $Q^\top \triangleq (p(n,j|m,i))_{(n,j),(m,i)\in\mathcal{CR}_1}$, where

$$\begin{aligned}p(n,j|m,i) &\triangleq P(X_t = n, C_t = j | X_{t-1} = m, C_{t-1} = i) \\ &= P(C_t = j | X_t = n, X_{t-1} = m, C_{t-1} = i) P(X_t = n | X_{t-1} = m, C_{t-1} = i) \\ &= \delta_{j,\max(0,n-w+i)} P(X_t = n | X_{t-1} = m).\end{aligned}$$

The initial probabilities are

$$\begin{aligned}p(n,j|c_0) &\triangleq P(X_1 = n, C_1 = j | C_0 = c_0) \\ &= P(C_1 = j | X_1 = n, C_0 = c_0) P(X_1 = n | C_0 = c_0) \\ &= \delta_{j,\max(0,n-w+c_0)} P(X_1 = n).\end{aligned}$$

Define the conditional probability that the run length of $\{X_t, C_t\}_{N_0}$ equals r by

$$p_{m,i}(r) \triangleq P((X_{r+1}, C_{r+1}) \notin \mathcal{CR}_1, (X_r, C_r), \cdots, (X_2, C_2) \in \mathcal{CR}_1 | (X_1, C_1) = (m,i)),$$

where $(m,i) \in \mathcal{CR}_1$. Let the vector $\mu_{(k)}$ denote the kth factorial moments that $(u_{(k)})_{m,i} \triangleq \sum_{r=1}^{\infty} r_{(k)} p_{m,i}(r)$ where $k \geq 1$ and $r_{(k)} = r \cdots (r-k+1)$. Then

$$p_{m,i}(r) = \sum_{(n,j)\in\mathcal{CR}_1} p_{n,j}(r-1) \cdot p(n,j|m,i),$$

$$(u_{(1)})_{m,i} = 1 + \sum_{(n,j)\in\mathcal{CR}_1} p(n,j|m,i) \cdot (u_{(1)})_{n,j}, \quad i.e., \quad (I-Q) \cdot u_{(1)} = 1.$$

The ARL is obtained as

$$ARL = \sum_{(m,i)\in\mathcal{CR}_1} (u_{(1)})_{m,i} \cdot p(m,i|c_0). \tag{3.1}$$

The above procedures can be carried out directly by Matlab. For simplicity we don't repeat the proof methods, see Weiß and Testik (2009) for more details.

The EWMA chart was first introduced by Roberts (1959). This chart weights samples following the rule of which the nearest samples in time series are weighted the most

while the previous samples contribute very little. Weiß (2009b) proposed a mixed-EWMA chart (a combination of a traditional Shewhart chart and EWMA chart) to detect persistent shifts for Poisson INAR processes. Weiß (2011) developed a single EWMA chart to monitor the Poisson INAR(1) process and proved that the single EWMA chart could be efficient and robust. The good performance of the single EWMA chart has also been verified in Zhang et al. (2014) and Li et al. (2019a). Thus the single EWMA chart is the second method used here. Let $Z_0 = z_0,\ z_0 \in N_0$, an EWMA statistic is given by $Z_t = \text{round}(hX_t + (1-h)Z_{t-1}),\ t \in N$, where $h \in (0,\ 1)$ is a constant, and round $(x) = z$ iff the integer $z \in (x - 1/2,\ x + 1/2]$. The details about the EWMA chart are given as follows:

Scheme 2 *(The EWMA chart). Let $UCL \in N$ with $UCL > 1$. The observations of $\{Z_t\}_{N_0}$ are plotted on an EWMA chart with control region $[0,\ UCL]$, i.e., the process is considered as being in control unless $Z_t > UCL$.*

The values of chart designs (h, UCL) are chosen such that the ARL_0 can be close to a given value (similar to the Scheme 1). The ARL computation method of the INAR-GIP(1) EWMA chart is also based on the Markov chain approach. Different from the CUSUM chart, the effective control region of the bivariate Markov process $\{X_t, Z_t\}_{N_0}$ is infinite and we cannot get the accurate values of ARL at this time. The control region is given by

$$\begin{aligned} \mathcal{CR}_2 &= \{(n,z) \in N_0 \times \{0,...,UCL\} | round(hn + (1-h)z) \in \{0,...,UCL\}\} \\ &= \{(n,z) | n \in N_0, z = \max(0, round(\lambda n)),...,\min(UCL,\ round((1-\lambda)UCL + \lambda n))\}. \end{aligned} \tag{3.2}$$

The approximate values of ARL can be obtained with arbitrary precision by choosing a sufficiently large limit of X_t. Similar approaches could be found in Weiß (2009b), the proof is also skipped for simplicity.

The combined jumps chart is the last method used here, which is a kind of mixed charts, combining the c-chart and the jump chart together. The c-chart is known as a kind of the most common Shewhart control charts, basing on the principles that the upper control limit and the lower control limit are computed as the mean of monitoring statistics plus and minus three times the standard deviation of monitoring statistics. The upper control limit of the c-chart is UCL (UCL $\in N$), and then plot $\{X_t\}$. If $X_t \notin [0,\ UCL]$,

the process is deemed to be out of control. Obviously, the c-chart handles the INAR(1) process the same as the i.i.d. process, regardless of the sequence autocorrelation. The jump chart proposed by Weiß (2009a) can better deal with the correlation of the process. The sample statistic jumps $J_t = X_t - X_{t-1}$ are plotted on a jump control chart with control region $[-k,\ k]$ for a $k > 0$; that is, the process is considered as being in control unless $|J_t| > k$. In terms of similar idea by Weiß (2009a), the combined jumps chart is also used to monitor the INAR-GIP(1) process.

Scheme 3 *(The combined jumps chart). Let $k,\ UCL \in N_0$ with $k \leqslant UCL$. The observed combined jumps $(X_t,\ J_t)_N$ are plotted in parallel on a c-chart with control region $[0,\ UCL]$ and a jump control chart with control region $[-k,\ k]$, i.e., the process is considered as being in control unless $X_t \notin [0,\ UCL]$ or $J_t \notin [-k,\ k]$.*

Obviously, the resulting control region of the combined jumps chart is included in $\{0, ..., UCL\} \times \{-k, ..., k\}$. In fact, it is given by

$$\begin{aligned} \mathcal{CR}_3 &= \{(n, j) \in \{0, ..., UCL\} \times \{-k, ..., k\} | n - j \in \{0, ..., UCL\}\} \\ &= \{(n, j) | n = 0, ..., UCL, j = \max(n - UCL, -k), ..., \min(n, k)\}. \end{aligned}$$

Markov chain approach for computing ARL of the combined jumps chart is also accepted. More details of the Markov chain approach for the combined jumps chart's ARL computation can be found in Weiß (2009a).

4 Numerical simulation

We will conduct some simulation studies to evaluate the finite sample performances of our proposed methods. First, we choose eight different combinations of $(\lambda,\ \alpha,\ \phi)$, and set $r = 6$. We compute the CML estimators for λ, α and ϕ with the help of Matlab. All the results are based on 1000 replications with the sample size $n = 100,\ 200,\ 500,$ and 1000, respectively. In Table 1, we report the estimated bias (BIAS) given by the sample mean of the estimate minus the true value, and the sampling standard error (SSE) of the estimate. The values are showed with the format BIAS(SE). For example, $-0.06094(0.03631)$ means that the BIAS is -0.06094 and SE is 0.03631. It can be seen from the results in Table 1 that the proposed CML estimators seem to be unbiased, and the performances become better as the sample size n increases.

As a comparision section, we conduct the second simulation to compare the performances of the CUSUM, EWMA and combined jumps charts in detecting changes of the process mean. In this paper, the in-control parameters of the INAR-GIP(1) process will be denoted as $\lambda_0,\ \alpha_0,\ \phi_0,\ r_0$. Moreover, when the process is in control, we donate the process mean μ_X as μ_0. As our main goal is to detect changes in μ_X, based on the previous description about the process, μ_X is exclusively influenced by parameter change of λ in the INAR-GIP(1) model, Table 2 shows some examples how change in μ_X effects the λ. So for the INAR-GIP(1) process, without loss of generality, we assume that changes only occur in λ, and the changes are sustained until an out-of-control signal is diagnosed. It is also necessary to know that the choice of initial values c_0 (z_0) in the CUSUM (EWMA) chart has a very small influence on the resulting ARLs (see Tables 3 and 4), hence, both c_0 and z_0 are fixed to 0 in the following computations and the results of ARL are shown with only two decimal places for simplicity. The mean upward shift magnitude $\delta_\mu = (\mu_X - \mu_0)/\mu_0$ is set as 5%, 10%, 20%, 30%, 40%, 50%, 60% and 70%, respectively. The desired in-control ARL value is equal to $\text{ARL}_0 = 370$. Moreover, besides ARL, we also adopt the usual relative deviation (in %) in the ARL (Weiß and Testik, 2011), $dev^{(\%)} = 100\% * (\text{ARL}-\text{ARL}_0)/\text{ARL}_0$ to evaluate the performances of control charts.

Figure 1 shows the ARL performance of the CUSUM charts with different values of chart designs. For example, for $(\mu_0, \alpha_0, \phi_0, r_0) = (1, 0.6, 0.6, 8)$ in Figure 1(a), there are three suitable sets of statistical designs leading to similar ARL_0, they are (w, UCL) = (1, 42), (2, 14) and (3, 8). From Figure 1 we can see that the CUSUM chart with smaller reference value of w shows a better sensitivity. Thus reference value w in the CUSUM chart is suggested to set as the smallest integer no less than μ_0, i.e., $\text{w} = \lceil \mu_0 \rceil$.

In Table 5, we study the CUSUM chart under $(\mu_0,\ \alpha_0) = (2,\ 0.3)$, (3, 0.4), (4, 0.5) with various values of $(\phi_0,\ r_0)$ respectively. The results show that the CUSUM chart is very efficient in detecting the upward shifts in μ_X. To be more specific, the values of ARL decrease when the process mean μ_X is increasing. Meanwhile, the decline proportion of ARL (absolute value of $dev^{(\%)}$) is much higher than the rise proportion of μ (δ_μ). Specifically, for $(\mu_0, \alpha_0, \phi_0, r_0) = (2, 0.3, 0, 6)$, when there is only 5% increasing in the process mean, the ARL drops significantly from 317.42 to 209.3. In this case, the out-of-control state will be identified as soon as the control chart alarms. Moreover, for

$(\mu_0, \alpha_0, \phi_0, r_0) = (2, 0.3, 0, 6)$, when the process mean increases from 2 to 3 ($\delta_\mu = 50\%$), the resulting ARL is only 33.98 ($dev^{(\%)} = -90.85\%$), which indicates that immediate alerts will arise in the CUSUM control chart. Similar conclusions also hold in other parameter combinations, so the CUSUM control chart works well for the INAR-GIP(1) process.

Table 6 shows the comparison of the EWMA charts with different sets of chart designs (h, UCL). It can be seen that different values of (h, UCL) will affect the efficiency of the chart and for h = 0.2 or 0.3, the EWMA chart performs better. As not every set of (h, UCL) will lead to an ARL_0 of about 370, for the EWMA control chart, we select the (h, UCL) with a smaller h on the premise that the corresponding ARL_0 is close to 370. In Table 7, we focus on assessing the performance of the EWMA chart. The results show that the EWMA chart is also effective in monitoring the mean shifts in INAR-GIP(1) process except for one parameters combination $(\mu_0,\ \alpha_0,\ \phi_0,\ r_0) = (2,\ 0.3,\ 0.8,\ 7)$.

In Figure 2, given a particular value of $(\mu_0,\ \alpha_0,\ \phi_0,\ r_0)$, we find that there is little difference in the sensitivity when the chart designs (k, UCL) of the combined jumps chart are different. Table 8 also clearly indicates that the combined jumps chart performs well in detecting the increasing shifts of μ_X with different in-control models. The analysis procedures are similar to those conclusions in Tables 5 and 7, and we omit the details.

Finally, Table 9 shows the comparison of three charts with different values of μ_0 (1, 3 and 5) in the INAR-GIP(1) process. The bold values show where the dev(%) is the smallest among three charts with the same model parameters. It becomes clear in Table 9 that each chart shows greater decrease ratio of ARL with the increasing of δ_μ. For the shift sizes of 5%, 10% and 20%, the CUSUM chart is consistently best in each combination of (μ_0, α_0). For shift sizes larger than $0.2\mu_0$, the sensitivity of three charts is nearly the same. As a whole, if the monitored data are from the INAR-GIP(1) process, the CUSUM chart is the best choice after various shift sizes are taken into consideration.

5 Real data analysis

In this section, we apply our proposed method to analyse the weekly telephone complaints data in Changchun (the capital of Jilin province in China). As the upward shifts in the process mean signify the decreasing of satisfaction, it should be quickly

identified. The data sets are collected in mayor's public telephone access project of Changchun. Our goal is to model and monitor these complaints data.

5.1 The first telephone complaints example

The first complaints data are about Changchun Water Conservancy Bureau. We consider the number of weekly telephone complaints from March 10th 2013 to August 30th 2015, which consists of 130 observations (see Figure 3). The first 100 observations are chosen as the Phase I samples, and the remaining series are used as the Phase II observations for control charts. From Figure 3, we can see that this data set appears to have mean shift. The sample mean and variance of the data (Phase I) are 3.47 and 4.8091, respectively. The autocorrelation function (ACF) and partial autocorrelation function (PACF) of these data (Phase I) are also reported in Figure 3, which indicate that $\{X_t\}$ may come from an AR(1)-type process. We consider the following six competitive models:

• INAR(1) model with Poisson marginal (Poisson INAR(1), Al-Osh and Alzaid, 1987);

• INAR(1) model with zero inflated Poisson innovations (ZIPINAR(1), Jazi et al., 2012);

• INAR(1) model with geometric marginal (GINAR(1), Alzaid and Al-Osh, 1988);

• New geometric INAR(1) model (NGINAR(1), Ristić et al., 2009);

• INAR(1) with negative binomial marginals (NBINAR(1), Ristić et al., 2012);

• Random coefficient INAR(1) model with negative binomial marginal (NBRCINAR(1), Weiß, 2008).

In Table 10, we summarize the estimated parameters, AIC and BIC for different models. From the results, the INAR-GIP(1) model has the smallest AIC and BIC. We can conclude that the INAR-GIP(1) model is the most appropriate for these data.

Below, we study the monitoring of complaints data based on the control charts. All the control chart designs should be selected that can result in the corresponding ARL_0 around 370 calculated with the estimated parameters. As more than one design combinations may be available each time, these different design combinations affect performance little, thus only one design combination result is presented here to improve the readability. For the lack of proper designs of the combined jumps chart leading to similar ARL_0, we only choose the following designs of the CUSUM and EWMA chart:

• The CUSUM chart design (w, UCL) = (4, 28), corresponding to $\text{ARL}_0 = 370.06$;

• The EWMA chart design (h, UCL) = (0.7, 9), corresponding to $\text{ARL}_0 = 389.6$.

Figure 4 shows two control charts with the telephone complaints data. Both charts do not trigger alarms at the Phase I. However, the alarms happen at $t = 113$ and $t \in [117, 130]$ in the CUSUM chart with Phase II. Similarly, the EWMA chart also alarms at $t = 113$ and $t = 124$. Based on our survey, an explanation for this phenomenon is that the domestic water pipes bursted during the last week of April in 2015 (corresponding to $t = 113$ in complaints data). The maintenance of the water pipes lasted about ten weeks, and the complaints towards the inconvenience still continued several weeks.

5.2 The second telephone complaints example

The second complaints data are about Changchun Tobacco Bureau, which consist of 123 observations starting from August 24th 2014 to December 25th 2016. The first 100 observations (from August 24th 2014 to July 17th 2016) are chosen as the Phase I samples (see Figure 5), and the remaining series are used as Phase II observations. The sample mean and variance (Phase I) are 2.15 and 3.0675, respectively. The ACF and PACF plots of the Phase I data are reported in Figure 5. We summarize the estimated parameters, AIC and BIC for different models in Table 11. It can be seen from the results that the INAR-GIP(1) model has the smallest AIC and BIC, which indicate that the INAR-GIP(1) model is the most appropriate.

The control charts are also used to monitor the complaints data, the selection method of the control limits is similar with the first example. We adopt the following two control charts:

- The CUSUM chart design (w, UCL) = (3, 12), corresponding to $\text{ARL}_0 = 341.12$;
- The EWMA chart design (h, UCL) = (0.2, 4), corresponding to $\text{ARL}_0 = 373.82$.

Based on the Figure 6, both control charts do not trigger alarms at Phases I and II, which indicate that the complaints data about Changchun Tobacco Bureau are in-control.

6 Concluding remarks

In this paper, we have proposed a new INAR-GIP(1) process which can model count time series data inflated at the $r + 1$ values $\{0, 1, \cdots, r\}$. Some statistical properties, together with the CML estimators of interested parameters were reported. Three popular control charts, the CUSUM, EWMA and combined jumps charts were applied to monitor

the process mean. Simulations and real data examples indiacted that the CUSUM chart was the most appropriate chart for the proposed INAR-GIP(1) model. Hence, we suggest to implement the CUSUM chart for practical application.

There exist several topics to be studied in our future research. First, our INAR-GIP(1) model is based on independent counting series. To make the model more flexible in analysing real data, it is desirable to consider a dependent counting series model as Ristić et al. (2013). Second, we can propose a new INAR-GIP(1) process with random coefficient α_t, and consider some related statistical inference topics. Third, it is interesting to extend our proposed INAR-GIP(1) process to p-th order, which can describe high-order dependence for count time series data. Fourth, we can consider a new bivariate INAR(1) process (Pedeli and Karlis, 2013) with geometrically inflated Poisson innovations. Fifth, under the complex system or uncertainty, the proposed chart can be extended under neutrosophic statistics (Albassam and Aslam, 2020; Aslam, 2020; Aslam and Albassam, 2020; Aslam et al., 2020 (a, b) and Shawky et al., 2020).

Acknowledgements

The authors wish to thank the Editor, the Associate Editor, and the reviewers for their many helpful and useful comments and suggestions that greatly improved the paper. This work is supported by National Natural Science Foundation of China (No. 11631003, 11690012, 11731015, 11871028, 11901053), Natural Science Foundation of Jilin Province (No. 20180101216JC), Program for Changbaishan Scholars of Jilin Province (2015010).

References

[1] Albassam, M. and Aslam, M. (2020). Monitoring non-conforming products using multiple dependent state sampling under indeterminacy-An application to juice industry. *IEEE Access*, 8, 172379-172386.

[2] Al-Osh, M. and Alzaid, A. (1987). First-order integer-valued autoregressive (INAR(1)) process. *Journal of Time Series Analysis*, **8**, 261-275.

[3] Alzaid, A. and Al-Osh, M. (1988). First-order integer-valued autoregressive (INAR(1)) process: distributional and regression properties. *Statistica Neerlandica*, **42**, 53-61.

[4] Aslam, M. (2020). Introducing Grubbs's test for detecting outliers under neutrosophic statistics-An application to medical data. *Journal of King Saud University-Science*, 32(6), 2696-2700.

[5] Aslam, M. and Albassam, M. (2020). Presenting post hoc multiple comparison tests under neutrosophic statistics. *Journal of King Saud University-Science*, 32(6), 2728-2732.

[6] Aslam, M., Al Shareef, A. and Khan, K. (2020a). Monitoring the temperature through moving average control under uncertainty environment. *Scientific Reports*, 10(1), 1-8.

[7] Aslam, M., Bantan, R. A.and Khan, N. (2020b). Design of NEWMA np control chart for monitoring neutrosophic nonconforming items. *Soft Computing*.

[8] Bakouch, H. S., Mohammadpour, M. and Shirozhan, M. (2018). A zero-inflated geometric INAR(1) process with random coefficient. *Applications of Mathematics*, **63**, 79-105.

[9] Bakouch, H. S. and Ristić, M. M. (2010). Zero truncated Poisson integer-valued AR(1) model. *Metrika*, **72**, 265-280.

[10] Barreto-Souza, W. (2015). Zero-modified geometric INAR(1) process for modelling count time series with deflation or inflation of zeros. *Journal of Time Series Analysis*, **36**, 839-852.

[11] Bourguignon, M., Borges, P. and Fajardo Molinares, F. (2018). A new geometric INAR(1) process based on counting series with deflation or inflation of zeros. *Journal of Statistical Computation and Simulation*, **88**, 3338-3348.

[12] Bourguignon, M., Rodrigues, J. and Santos-Neto, M. (2019). Extended Poisson INAR (1) processes with equidispersion, underdispersion and overdispersion. *Journal of Applied Statistics*, **46**, 101-118.

[13] Cabral Morais, M. and Knoth, S. (2020). Improving the ARL profile and the accuracy of its calculation for Poisson EWMA charts. *Quality and Reliability Engineering International*, **36**, 876-889.

[14] Darolles, S., Le Fol, G., Lu, Y. and Sun, R. (2019). Bivariate integer-autoregressive process with an application to mutual fund flows. *Journal of Multivariate Analysis*, **173**, 181-203.

[15] Fernández-Fontelo, A., Cabaña, A., Joe, H., Puig, P. and Moriña, D. (2019). Untangling serially dependent underreported count data for gender-based violence. *Statistics in Medicine*, **38**, 4404-4422.

[16] Heathcote, C. (1966). Corrections and comments on the paper "A branching process allowing immigration". *Journal of the Royal Statistical Society: Series B (Methodological)*, **28**, 213-217.

[17] Jazi, M., Jones, G. and Lai, C. (2012). First-order integer valued AR processes with zero inflated Poisson innovations. *Journal of Time Series Analysis*, **33**, 954-963.

[18] Jentsch, C. and Weiß, C. H. (2019). Bootstrapping INAR models. *Bernoulli*, **25**, 2359-2408.

[19] Kang, Y., Wang, D. and Yang, K. (2019). A new INAR(1) process with bounded support for counts showing equidispersion, underdispersion and overdispersion. *Statistical Papers*, DOI: 10.1007/s00362-019-01111-0.

[20] Kim, H. and Lee, S. (2019). Improved CUSUM monitoring of Markov counting process with frequent zeros. *Quality and Reliability Engineering International*, **35**, 2371-2394.

[21] Lu, Y. (2019). The predictive distributions of thinning-based count processes. *Scandinavian Journal of Statistics*, DOI: 10.1111/sjos.12438.

[22] Li, C., Wang, D. and Zhang, H. (2015). First-order mixed integer-valued autoregressive processes with zero-inflated generalized power series innovations. *Journal of the Korean Statistical Society*, **44**, 232-246.

[23] Li, C., Wang, D. and Zhu, F. (2016). Effective control charts for monitoring the NGINAR(1) process. *Quality and Reliability Engineering International*, **32**, 877-888.

[24] Li, C., Wang, D. and Zhu, F. (2019a). Detecting mean increases in zero truncated INAR(1) processes. *International Journal of Production Research*, **57**, 5589-5603.

[25] Li, C., Wang, D. and Sun, J. (2019b). Control charts based on dependent count data with deflation or inflation of zeros. *Journal of Statistical Computation and Simulation*, **89**, 3273-3289.

[26] Li, J., Zhou, Q. and Ding, D. (2020). Efficient monitoring of autocorrelated Poisson counts. *IISE Transactions*, **52**, 769-779.

[27] Möller, T. A., Weiß, C. H., Kim, H. Y. and Sirchenko, A. (2018). Modeling zero inflation in count data time series with bounded support. *Methodology and Computing in Applied Probability*, **20**, 589-609.

[28] Möller, T. A., Weiß, C. H. and Kim, H. Y. (2020). Modelling counts with state-dependent zero inflation. *Statistical Modelling*, **20**, 127-147.

[29] Nastić, A., Laketa, P. and Ristić, M. (2016). Random environment integer-valued autoregressive process. *Journal of Time Series Analysis*, **37**, 267-287.

[30] Page, E. (1961). Cumulative sum charts. *Technometrics*, **3**, 1-9.

[31] Pedeli, X. and Karlis, D. (2013). Some properties of multivariate INAR(1) processes. *Computational Statistics and Data Analysis*, **67**, 213-225.

[32] Rakitzis, A. C., Castagliola, P. and Maravelakis, P. E. (2016). A two-parameter general inflated Poisson distribution: Properties and applications. *Statistical Methodology*, **29**, 32-50.

[33] Rakitzis, A. C., Castagliola, P. and Maravelakis, P. E. (2018). Cumulative sum control charts for monitoring geometrically inflated Poisson processes: An application to infectious disease counts data. *Statistical Methods in Medical Research*, **27**, 622-641.

[34] Rakitzis, A. C., Weiß, C. H. and Castagliola, P. (2017). Control charts for monitoring correlated Poisson counts with an excessive number of zeros. *Quality and Reliability Engineering International*, **33**, 413-430.

[35] Ristić, M., Bakouch, H. and Nastić, A. (2009). A new geometric first-order integer-valued autoregressive (NGINAR(1)) process. *Journal of Statistical Planning and Inference*, **139**, 2218-2226.

[36] Ristić, M., Nastić, A. and Bakouch, H. (2012). Estimation in an integer-valued autoregressive process with negative binomial marginals (NBINAR(1)). *Communications in Statistics-Theory and Methods*, **41**, 606-618.

[37] Ristić, M., Nastić, A. and Miletić llić, A. (2013). A geometric time series model with dependent Bernoulli counting series. *Journal of Time Series Analysis*, **34**, 466-476.

[38] Roberts, S. (1959). Control chart tests based on geometric moving averages. *Technometrics*, **1**, 239-250.

[39] Sales, L. O., Pinho, A. L., Vivacqua, C. A. and Ho, L. L. (2020). Shewhart control chart for monitoring the mean of Poisson mixed integer autoregressive processes via Monte Carlo simulation. *Computers and Industrial Engineering*, **140**, 106245.

[40] Schweer, S. and Weiß, C. H. (2014). Compound Poisson INAR(1) processes: Stochastic properties and testing for overdispersion. *Computational Statistics and Data Analysis*, **77**, 267-284.

[41] Scotto, M., Weiß, C. H. and Gouveia, S. (2015). Thinning-based models in the analysis of integer-valued time series: a review. *Statistical Modelling*, **15**, 590-618.

[42] Sellers, K. F., Peng, S. J. and Arab, A. (2020). A flexible univariate autoregressive time-series model for dispersed count Data. *Journal of Time Series Analysis*, **41**, 436-453.

[43] Shamma, N., Mohammadpour, M. and Shirozhan, M. (2020). A time series model based on dependent zero inflated counting series. *Computational Statistics*, doi: 10.1007/s00180-020-00982-4.

[44] Shawky, A. I., Aslam, M. and Khan, K. (2020). Multiple dependent state sampling-based chart using belief statistic under neutrosophic statistics. *Journal of Mathematics*, 2020.

[45] Steutel, F. and Van Harn, K. (1979). Discrete Analogues of Self-Decomposability and Stability. *Annals of Probability*, **7**, 893-899.

[46] Vanli, O. A., Giroux, R., Erman Ozguven, E. and Pignatiello Jr, J. J. (2019). Monitoring of count data time series: Cumulative sum change detection in Poisson integer valued GARCH models. *Quality Engineering*, **31**, 439-452.

[47] Weiß, C. H. (2008). Thinning operations for modeling time series of counts-a survey. *Advances in Statistical Analysis*, **92**, 319-341.

[48] Weiß, C. H. (2009a). Controlling jumps in correlated processes of Poisson counts. *Applied Stochastic Models in Business and Industry*, **25**, 551-564.

[49] Weiß, C. H. (2009b). EWMA monitoring of correlated processes of Poisson counts. *Quality Technology and Quantitative Management*, **6**, 137-153.

[50] Weiß, C. H. (2011). Detecting mean increases in Poisson INAR(1) processes with EWMA control charts. *Journal of Applied Statistics*, **38**, 383-398.

[51] Weiß, C. H. (2015). SPC methods for time-dependent processes of counts-A literature review. *Cogent Mathematics*, **2**, 1111116.

[52] Weiß, C. H., Homburg, A. and Puig, P. (2019). Testing for zero inflation and overdispersion in INAR(1) models. *Statistical Papers*, **60**, 473-498.

[53] Weiß, C. H. and Testik, M. (2009). CUSUM monitoring of first-order integer-valued autoregressive processes of Poisson counts. *Journal of Quality Technology*, **41**, 389-400.

[54] Weiß, C. H. and Testik, M. (2011). The Poisson INAR(1) CUSUM chart under overdispersion and estimation error. *IIE Transactions*, **43**, 805-818.

[55] Xie, M., He, B. and Goh, T. (2001). Zero-inflated Poisson model in statistical process control. *Computational Statistics and Data Analysis*, **38**, 191-201.

[56] Yontay, P., Weiß, C. H., Testik, M. C. and Bayindir, Z. (2013). A two-sided cumulative sum chart for first-order integer-valued autoregressive processes of poisson counts. *Quality and Reliability Engineering International*, **29**, 33-42.

[57] Zhang, M., Nie, G., He, Z. and Hou, X. (2014). The Poisson INAR(1) one-sided EWMA chart with estimated parameters. *International Journal of Production Research*, **52**, 5415-5431.

[58] Zhang, H., Wang, D. and Zhu, F. (2010). Inference for INAR(p) processes with signed generalized power series thinning operator. *Journal of Statistical Planning and Inference*, **140**, 667-683.

[59] Zhang, H., Wang, D. and Zhu, F. (2012). Generalized RCINAR(1) process with signed thinning operator. *Communications in Statistics: Theory and Methods*, **41**, 1750-1770.

[60] Zheng, H., Basawa, I. and Datta, S. (2007). First-order random coefficient integer-valued autoregressive processes. *Journal of Statistical Planning and Inference*, **137**, 212-229.

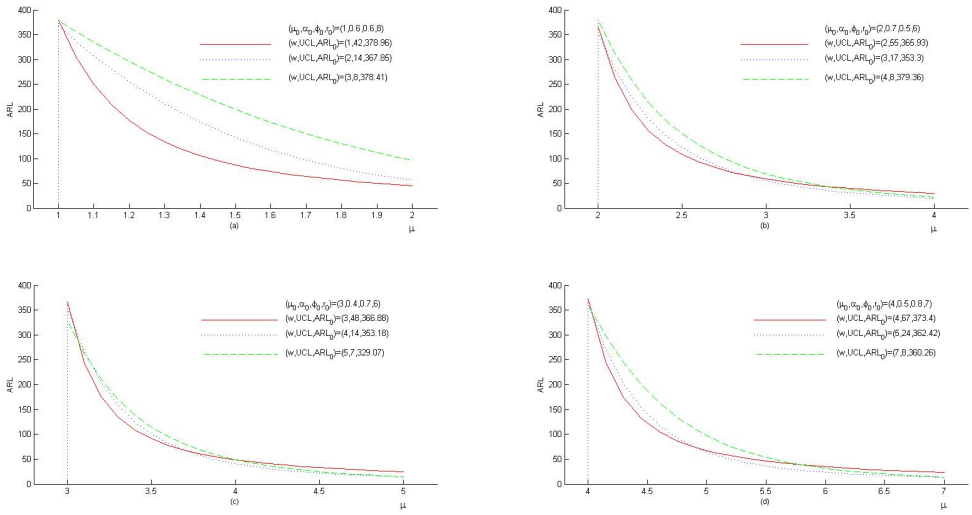

Figure 1. ARLs of the CUSUM chart under different chart designs (w, UCL).

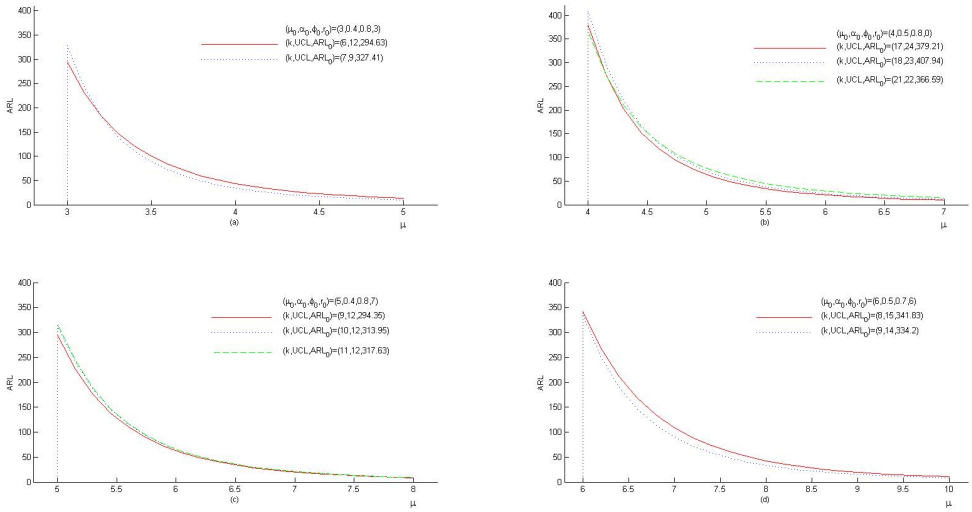

Figure 2. ARLs of the combined jumps chart under different chart designs (k, UCL).

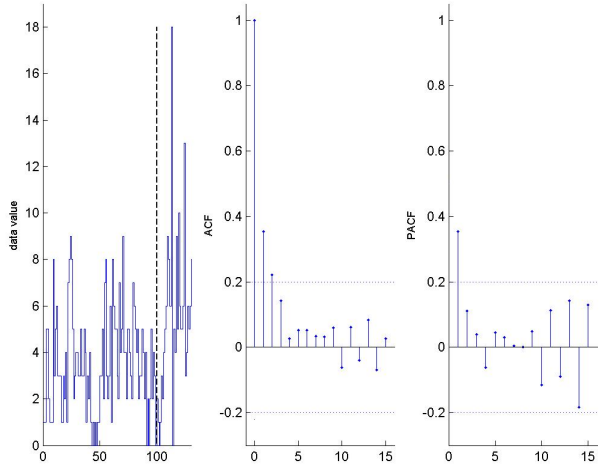

Figure 3. Sample path, ACF plot, and PACF plot for the weekly telephone complaints of Water Conservancy Bureau.

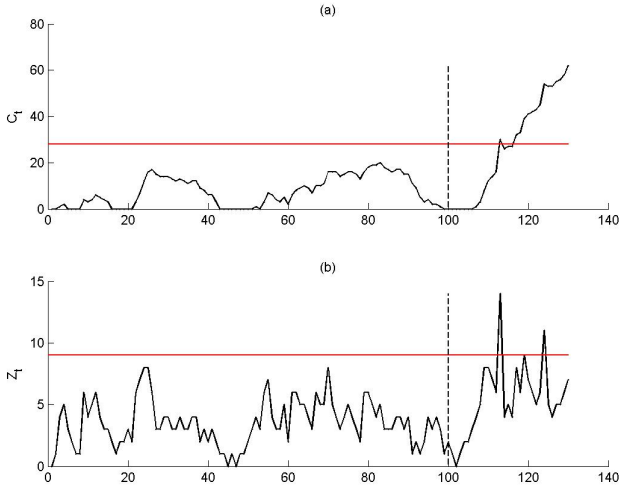

Figure 4. (a) CUSUM chart with (w, UCL) = (4, 28); (b) EWMA chart with (h, UCL) = (0.7, 9) for the weekly telephone complaints of Water Conservancy Bureau.

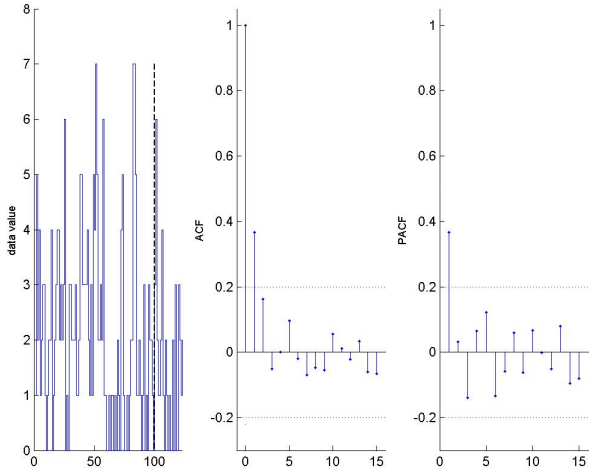

Figure 5. Sample path, ACF plot, and PACF plot for the weekly telephone complaints of Tobacco Bureau.

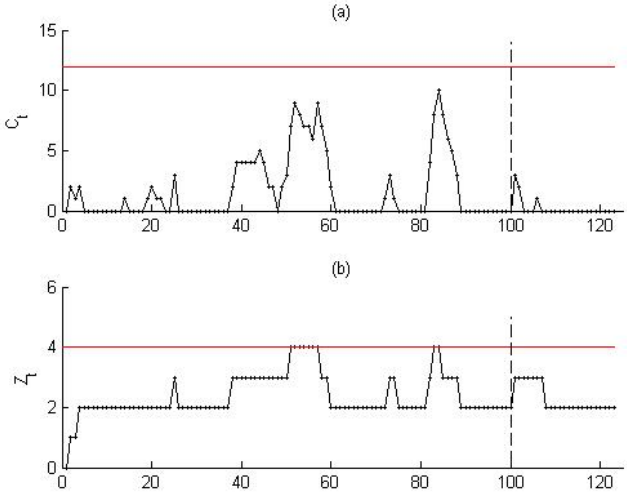

Figure 6. (a) CUSUM chart with (w, UCL) = (3, 12); (b) EWMA chart with (h, UCL) = (0.63, 6) for the weekly telephone complaints of Tobacco Bureau.

Table 1. The BIAS and SSE of estimates with r=6[‡].

n	$\hat{\lambda}$	$\hat{\alpha}$	$\hat{\phi}$	$\hat{\lambda}$	$\hat{\alpha}$	$\hat{\phi}$
	True values $\lambda = 1$, $\alpha = 0.3$, $\phi = 0.4$.			True values $\lambda = 2$, $\alpha = 0.4$, $\phi = 0.4$.		
100	-0.06094(0.03631)	0.00033(0.00703)	0.07168(0.02767)	-0.10066(0.15602)	-0.00368(0.00666)	0.15068(0.07238)
200	-0.04416(0.01788)	-0.00023(0.00402)	0.05415(0.02039)	-0.08289(0.06813)	0.00617(0.00303)	0.10959(0.05821)
500	-0.02578(0.00725)	0.00037(0.00156)	0.02453(0.01603)	-0.02304(0.0227)	-0.00148(0.00133)	0.04088(0.04384)
1000	-0.01682(0.00329)	0.00047(0.00077)	0.00068(0.01452)	-0.02329(0.01065)	0.00028(0.0007)	0.02335(0.03455)
	True values $\lambda = 1$, $\alpha = 0.3$, $\phi = 0.5$.			True values $\lambda = 2$, $\alpha = 0.4$, $\phi = 0.5$.		
100	-0.05387(0.03721)	0.00043(0.00704)	0.01137(0.02035)	-0.16336(0.17829)	0.00329(0.00625)	0.08072(0.04932)
200	-0.02955(0.01897)	-0.00573(0.00429)	-0.00405(0.01575)	-0.11338(0.08121)	0.00116(0.00308)	0.05812(0.04562)
500	-0.01497(0.00751)	0.00096(0.00159)	-0.02269(0.01337)	-0.05229(0.02851)	-0.00222(0.00147)	-0.01268(0.03928)
1000	-0.006 (0.004)	-0.00054(0.00088)	-0.01745(0.00851)	-0.03379(0.01204)	-0.00156(0.00073)	-0.02497(0.03087)
	True values $\lambda = 1$, $\alpha = 0.3$, $\phi = 0.6$.			True values $\lambda = 2$, $\alpha = 0.4$, $\phi = 0.6$.		
100	-0.03952(0.04742)	-0.00695(0.00673)	-0.01341(0.01482)	-0.17053(0.19228)	-0.00083(0.00624)	0.01654(0.04142)
200	-0.006 (0.02137)	-0.00326(0.00363)	-0.02479(0.01259)	-0.09444(0.08169)	-0.00273(0.00347)	-0.018(0.03891)
500	0.00407(0.00972)	-0.00205(0.00155)	-0.01893(0.00549)	-0.05662(0.03296)	-0.00134(0.00132)	-0.0509(0.03687)
1000	0.00344(0.00535)	-0.00248(0.00079)	-0.00926(0.00257)	-0.03233(0.01468)	-0.00233(0.0007)	-0.05154(0.02868)
	True values $\lambda = 1$, $\alpha = 0.3$, $\phi = 0.8$.			True values $\lambda = 2$, $\alpha = 0.4$, $\phi = 0.7$.		
100	0.04329(0.12146)	-0.00477(0.00603)	-0.01949(0.0054)	-0.14594(0.20933)	-0.00371(0.00618)	-0.03867(0.04028)
200	0.01025(0.05828)	-0.0034(0.00327)	-0.00758(0.00138)	-0.11235(0.10539)	0.00122(0.003)	-0.04143(0.03231)
500	0.00583(0.02381)	-0.00029(0.00119)	-0.00201(0.00047)	-0.02936(0.04143)	-0.00406(0.00132)	-0.0518(0.02716)
1000	0.00311(0.01076)	-0.00034(0.00064)	-0.00228(0.00021)	-0.01488(0.02204)	-0.00169(0.00062)	-0.03758(0.01673)

[‡] The SSE is in parenthesis.

Table 2. The relationship between μ_X and λ.

	$\phi = 0.3,\ r = 2,\ \alpha = 0.3$								
	$\mu_X = 1$	$\mu_X = 1.05$	$\mu_X = 1.1$	$\mu_X = 1.2$	$\mu_X = 1.3$	$\mu_X = 1.4$	$\mu_X = 1.5$	$\mu_X = 1.6$	$\mu_X = 1.7$
λ	0.7573	0.7979	0.8386	0.9199	1.0012	1.0825	1.1638	1.2451	1.3264
	$\phi = 0.4,\ r = 6,\ \alpha = 0.3$								
	$\mu_X = 2$	$\mu_X = 2.1$	$\mu_X = 2.2$	$\mu_X = 2.4$	$\mu_X = 2.6$	$\mu_X = 2.8$	$\mu_X = 3$	$\mu_X = 3.2$	$\mu_X = 3.4$
λ	1.4783	1.5556	1.6330	1.7877	1.9424	2.0971	2.2518	2.4065	2.5612
	$\phi = 0.7,\ r = 6,\ \alpha = 0.4$								
	$\mu_X = 3$	$\mu_X = 3.15$	$\mu_X = 3.3$	$\mu_X = 3.6$	$\mu_X = 3.9$	$\mu_X = 4.2$	$\mu_X = 4.5$	$\mu_X = 4.8$	$\mu_X = 5.1$
λ	1.8418	1.9715	2.1011	2.3605	2.6198	2.8791	3.1384	3.3977	3.6571
	$\phi = 0.8,\ r = 7,\ \alpha = 0.5$								
	$\mu_X = 4$	$\mu_X = 4.2$	$\mu_X = 4.4$	$\mu_X = 4.8$	$\mu_X = 5.2$	$\mu_X = 5.6$	$\mu_X = 6$	$\mu_X = 6.4$	$\mu_X = 6.8$
λ	1.7240	1.8953	2.0666	2.4091	2.7516	3.0942	3.4367	3.7792	4.1218
	$\phi = 0.5,\ r = 7,\ \alpha = 0.5$								
	$\mu_X = 5$	$\mu_X = 5.25$	$\mu_X = 5.5$	$\mu_X = 6$	$\mu_X = 6.5$	$\mu_X = 7$	$\mu_X = 7.5$	$\mu_X = 8$	$\mu_X = 8.5$
λ	2.7178	2.8606	3.0033	3.2889	3.5745	3.86	4.1456	4.4311	4.7167

Table 3. ARL_0 of the CUSUM chart in different in-control processes with different c_0.

	$\mu_0 = 1$ $\alpha_0 = 0.6$ $\phi_0 = 0.6$ $r_0 = 8$ w=3 UCL=8	$\mu_0 = 2$ $\alpha_0 = 0.7$ $\phi_0 = 0.5$ $r_0 = 6$ w=4 UCL=8	$\mu_0 = 3$ $\alpha_0 = 0.4$ $\phi_0 = 0.7$ $r_0 = 6$ w=4 UCL=14	$\mu_0 = 4$ $\alpha_0 = 0.5$ $\phi_0 = 0.8$ $r_0 = 7$ w=5 UCL=24	$\mu_0 = 5$ $\alpha_0 = 0.5$ $\phi_0 = 0.5$ $r_0 = 7$ w=6 UCL=24
$c_0 = 0$	378.33	379.44	353.18	362.42	351.74
$c_0 = 1$	377.82	378.59	352.37	361.84	351.12
$c_0 = 2$	377.04	377.24	351.16	361.11	350.34
$c_0 = 3$	375.58	375.37	349.37	360.17	349.43
$c_0 = 4$	373.81	373.05	347.08	358.97	348.15
$c_0 = 5$	371.09	369.03	344.12	357.51	346.68
$c_0 = 6$	366.99	364.34	340.04	355.77	344.99

Table 4. ARL_0 of the EWMA chart in different in-control processes with different z_0.

	$\mu_0 = 1$ $\alpha_0 = 0.6$ $\phi_0 = 0.6$ $r_0 = 8$ h=0.5 UCL=5	$\mu_0 = 2$ $\alpha_0 = 0.7$ $\phi_0 = 0.5$ $r_0 = 6$ h=0.4 UCL=5	$\mu_0 = 3$ $\alpha_0 = 0.4$ $\phi_0 = 0.7$ $r_0 = 6$ h=0.2 UCL=5	$\mu_0 = 4$ $\alpha_0 = 0.5$ $\phi_0 = 0.8$ $r_0 = 7$ h=0.7 UCL=10	$\mu_0 = 5$ $\alpha_0 = 0.5$ $\phi_0 = 0.5$ $r_0 = 7$ h=0.8 UCL=11
$z_0 = 0$	352.86	414.31	364.76	422.56	316.54
$z_0 = 1$	352.29	413.83	363.22	422.43	316.55
$z_0 = 2$	351.55	413.02	360.82	422.29	316.28
$z_0 = 3$	350.81	412.1	357.17	422.03	316.33
$z_0 = 4$	349.27	410.35	350.98	421.96	316.18

Table 5. The performances of ARL and dev$^{(\%)}$ with the CUSUM charts‡.

$\mu_0 = 2,\ \alpha_0 = 0.3$						
δ_μ	$\phi_0 = 0,\ r_0 = 6$	$\phi_0 = 0.4,\ r_0 = 6$	$\phi_0 = 0.7,\ r_0 = 6$	$\phi_0 = 0.8,\ r_0 = 0$	$\phi_0 = 0.8,\ r_0 = 3$	$\phi_0 = 0.8,\ r_0 = 7$
0	371.42	374.03	375.15	371.58	365.32	366.83
5%	209.3 (-43.65%)	212.56 (-43.17%)	223.36 (-40.46%)	272.88 (-26.56%)	205.08 (-43.86%)	243.78 (-33.54%)
10%	138.53 (-62.7%)	141.33 (-62.21%)	151.23 (-59.69%)	212.04 (-42.94%)	135.96 (-62.78%)	174.12 (-52.53%)
20%	79.76 (-78.53%)	81.7 (-78.16%)	88.34 (-76.45%)	143.72 (-61.32%)	78.68 (-78.46%)	105.61 (-71.21%)
30%	55.33 (-85.1%)	56.78 (-84.82%)	61.52 (-83.6%)	107.59 (-71.05%)	54.8 (-85%)	74.29 (-79.75%)
40%	42.17 (-88.65%)	43.33 (-88.42%)	46.96 (-87.48%)	85.69 (-76.94%)	41.94 (-88.52%)	56.9 (-84.49%)
50%	33.98 (-90.85%)	34.94 (-90.66%)	37.89 (-89.9%)	71.14 (-80.85%)	33.93 (-90.71%)	45.92 (-87.48%)
60%	28.39 (-92.36%)	29.22 (-92.19%)	31.69 (-91.55%)	60.78 (-83.64%)	28.46 (-92.21%)	38.42 (-89.53%)
70%	24.36 (-93.44%)	25.08 (-93.29%)	27.21 (-92.75%)	53.09 (-85.71%)	24.52 (-93.29%)	32.97 (-91.01%)
UCL	33	34	37	77	33	45
w	2	2	2	2	2	2
$\mu_0 = 3,\ \alpha_0 = 0.4$						
δ_μ	$\phi_0 = 0,\ r_0 = 6$	$\phi_0 = 0.4,\ r_0 = 6$	$\phi_0 = 0.7,\ r_0 = 6$	$\phi_0 = 0.8,\ r_0 = 0$	$\phi_0 = 0.8,\ r_0 = 3$	$\phi_0 = 0.8,\ r_0 = 7$
0	373.6	379.89	366.87	368.91	373.95	370.17
5%	201.16 (-46.16%)	206.57 (-45.62%)	205.67 (-43.94%)	269.78 (-26.87%)	205.74 (-44.98%)	221.63 (-40.13%)
10%	130.34 (-65.11%)	134.54 (-64.58%)	135.61 (-63.04%)	209.07 (-43.33%)	135.6 (-63.74%)	149.83 (-59.52%)
20%	73.81 (-80.24%)	76.57 (-79.84%)	77.77 (-78.8%)	141.37 (-61.68%)	78.25 (-79.07%)	87.04 (-76.49%)
30%	50.87 (-86.38%)	52.89 (-86.08%)	53.83 (-85.33%)	105.7 (-71.35%)	54.51 (-85.42%)	60.38 (-83.69%)
40%	38.6 (-89.67%)	40.2 (-89.42%)	40.96 (-88.84%)	84.15 (-77.19%)	41.71 (-88.85%)	45.95 (-87.59%)
50%	31 (-91.7%)	32.32 (-91.49%)	32.97 (-91.01%)	69.83 (-81.07%)	33.76 (-90.97%)	36.98 (-90.01%)
60%	25.84 (-93.08%)	26.99 (-92.9%)	27.55 (-92.49%)	59.69 (-83.82%)	28.35 (-92.42%)	30.89 (-91.66%)
70%	22.12 (-94.08%)	23.12 (-93.91%)	23.63 (-93.56%)	52.12 (-85.87%)	24.42 (-93.47%)	26.48 (-92.85%)
UCL	45	47	48	112	49	54
w	3	3	3	3	3	3
$\mu_0 = 4,\ \alpha_0 = 0.5$						
δ_μ	$\phi_0 = 0,\ r_0 = 6$	$\phi_0 = 0.4,\ r_0 = 6$	$\phi_0 = 0.7,\ r_0 = 6$	$\phi_0 = 0.8,\ r_0 = 0$	$\phi_0 = 0.8,\ r_0 = 3$	$\phi_0 = 0.8,\ r_0 = 7$
0	373.47	371.51	372.28	370.9	375.72	373.39
5%	199.03 (-46.71%)	201.32 (-45.81%)	204.8 (-44.99%)	265.72 (-28.36%)	208.22 (-44.58%)	215.49 (-42.29%)
10%	128.23 (-65.67%)	130.81 (-64.79%)	133.96 (-64.02%)	200.18 (-46.03%)	137.74 (-63.34%)	143.27 (-61.63%)
20%	72.25 (-80.65%)	74.26 (-80.01%)	76.34 (-79.49%)	127.31 (-65.68%)	79.7 (-78.79%)	82.24 (-77.97%)
30%	49.63 (-86.71%)	51.15 (-86.23%)	52.72 (-85.84%)	90.19 (-75.68%)	55.55 (-85.22%)	56.79 (-84.79%)
40%	37.57 (-89.94%)	38.8 (-89.56%)	40.03 (-89.25%)	68.72 (-81.47%)	42.53 (-88.68%)	43.14 (-88.45%)
50%	30.12 (-91.94%)	31.16 (-91.61%)	32.18 (-91.36%)	55.05 (-85.16%)	34.39 (-90.85%)	34.68 (-90.71%)
60%	25.07 (-93.29%)	25.97 (-93.01%)	26.85 (-92.79%)	45.78 (-87.66%)	28.88 (-92.31%)	28.93 (-92.25%)
70%	21.42 (-94.26%)	22.22 (-94.02%)	23.02 (-93.82%)	39.13 (-89.45%)	24.88 (-93.38%)	24.78 (-93.36%)
UCL	58	60	62	85	66	67
w	4	4	4	5	4	4

‡ The dev$^{(\%)}$ is in parenthesis.

Table 6. ARLs of the EWMA chart under different chart designs (h, UCL)[‡] .

δ_μ	$\mu_0 = 2,\ \alpha_0 = 0.4,\ \phi_0 = 0.7,\ r_0 = 6$								
0	356.6	474.26	840.71	440.53	463	484.11	1008.69	658.21	1035.41
5%	319.75	387.01	680.92	367.99	391.05	413.62	875.97	572.53	910.17
	(-10.33%)	(-18.4%)	**(-19.01%)**	(-16.47%)	(-15.54%)	(-14.56%)	(-13.16%)	(-13.02%)	(-12.1%)
10%	285.14	315.06	549.77	306.37	328.73	351.3	754.24	494.22	793.33
	(-20.04%)	(-33.57%)	**(-34.61%)**	(-30.45%)	(-29%)	(-27.43%)	(-25.23%)	(-24.91%)	(-23.38%)
20%	223.48	209.08	357.13	211.32	230.21	250.07	546.77	360.99	589
	(-37.33%)	(-55.91%)	**(-57.52%)**	(-52.03%)	(-50.28%)	(-48.34%)	(-45.79%)	(-45.16%)	(-43.11%)
30%	172.41	140.72	233.28	146.06	160.61	176.33	387.43	258.47	426.29
	(-51.65%)	(-70.33%)	**(-72.25%)**	(-66.84%)	(-65.31%)	(-63.58%)	(-61.59%)	(-60.73%)	(-58.83%)
40%	131.96	97.13	154.94	102.1	112.75	124.42	271.16	183.37	303.48
	(-62.99%)	(-79.52%)	**(-81.57%)**	(-76.82%)	(-75.65%)	(-74.3%)	(-73.12%)	(-72.14%)	(-70.69%)
50%	101.06	69.19	105.5	72.72	80.29	88.65	189.45	130.25	214.73
	(-71.66%)	(-85.41%)	**(-87.45%)**	(-83.49%)	(-82.66%)	(-81.69%)	(-81.22%)	(-80.21%)	(-79.26%)
60%	77.95	51	74.04	52.99	58.33	64.25	133.4	93.36	152.47
	(-78.14%)	(-89.25%)	**(-91.19%)**	(-87.97%)	(-87.4%)	(-86.73%)	(-86.77%)	(-85.82%)	(-85.27%)
70%	60.86	38.87	53.66	39.63	43.36	47.53	95.32	68.08	109.51
	(-82.93%)	(-91.8%)	**(-93.62%)**	(-91%)	(-90.63%)	(-90.18%)	(-90.55%)	(-89.66%)	(-89.42%)
UCL	3	4	5	5	6	6	7	7	8
h	0.1	0.2	0.3	0.4	0.5	0.6	0.7	0.8	0.9
δ_μ	$\mu_0 = 3,\ \alpha_0 = 0.5,\ \phi_0 = 0.8,\ r_0 = 7$								
0	1039.53	481.3	553	871.74	724.75	639.97	351.4	650.6	348.31
5%	896.78	396.27	464.12	749.27	634.51	568.77	317.88	590.92	318.66
	(-13.73%)	**(-17.67%)**	(-16.07%)	(-14.05%)	(-12.45%)	(-11.13%)	(-9.54%)	(-9.17%)	(-8.51%)
10%	767.27	325.04	387.57	639.22	551.5	501.91	285.66	532.71	289.67
	(-26.19%)	**(-32.47%)**	(-29.92%)	(-26.67%)	(-23.9%)	(-21.57%)	(-18.71%)	(-18.12%)	(-16.84%)
20%	550.11	217.57	267.1	455.78	407.7	382.01	225.73	422.47	233.79
	(-47.08%)	**(-54.8%)**	(-51.7%)	(-47.72%)	(-43.75%)	(-40.31%)	(-35.76%)	(-35.06%)	(-32.88%)
30%	386.83	146.11	182.46	317.58	293.62	282.49	173.64	324.13	183.26
	(-62.79%)	**(-69.64%)**	(-67.01%)	(-63.57%)	(-59.49%)	(-55.86%)	(-50.59%)	(-50.18%)	(-47.39%)
40%	270.13	99.61	124.85	218.04	207.25	203.87	130.41	240.99	139.91
	(-74.01%)	**(-79.3%)**	(-77.42%)	(-74.99%)	(-71.4%)	(-68.14%)	(-62.89%)	(-62.96%)	(-59.83%)
50%	189.66	69.67	86.45	149.12	144.82	144.85	96.41	174.76	104.72
	(-81.76%)	**(-85.52%)**	(-84.37%)	(-82.89%)	(-80.02%)	(-77.37%)	(-72.56%)	(-73.14%)	(-69.93%)
60%	135.32	50.29	61.12	102.7	101.24	102.38	70.76	124.89	77.44
	(-86.98%)	**(-89.55%)**	(-88.95%)	(-88.22%)	(-86.03%)	(-84%)	(-79.86%)	(-80.8%)	(-77.77%)
70%	98.73	37.59	44.42	71.96	71.55	72.78	52.04	88.95	57.14
	(-90.5%)	**(-92.19%)**	(-91.97%)	(-91.75%)	(-90.13%)	(-88.63%)	(-85.19%)	(-86.33%)	(-83.6%)
UCL	6	6	7	8	9	9	9	10	10
h	0.1	0.2	0.3	0.4	0.5	0.6	0.7	0.8	0.9

[‡]The dev$^{(\%)}$ is in parenthesis.

Table 7. The performances of ARL and dev$^{(\%)}$ with EWMA charts‡.

$\mu_0 = 2,\ \alpha_0 = 0.3$						
δ_μ	$\phi_0 = 0,\ r_0 = 6$	$\phi_0 = 0.4,\ r_0 = 6$	$\phi_0 = 0.7,\ r_0 = 6$	$\phi_0 = 0.8,\ r_0 = 0$	$\phi_0 = 0.8,\ r_0 = 3$	$\phi_0 = 0.8,\ r_0 = 7$
0	419.94	363.28	407.52	331.58	397.97	352.64
5%	299.75 (-28.62%)	260.88 (-28.19%)	342.64 (-15.92%)	241.85 (-27.06%)	260.6 (-34.52 %)	334.6 (-5.12%)
10%	219.52 (-47.73%)	192.16 (-47.1%)	286.04 (-29.81%)	182.34 (-45.01%)	177.44 (-55.41%)	316.71 (-10.19%)
20%	126.11 (-69.97%)	111.64 (-69.27%)	196.51 (-51.78%)	112.61 (-66.04%)	91.5 (-77.01%)	281.45(-20.19%)
30%	78.47 (-81.31%)	70.26 (-80.66%)	134.08 (-67.1%)	76.06 (-77.06%)	53.24 (-86.62%)	246.5 (-30.1%)
40%	52.22 (-87.56 %)	47.27 (-86.99%)	92.14 (-77.39%)	55.04 (-83.4%)	34.1(-91.43%)	211.83(-39.93 %)
50%	36.78 (-91.24%)	33.65 (-90.74%)	64.44 (-84.19%)	42.01 (-87.33%)	23.56 (-94.08%)	178.07 (-49.5%)
60%	27.15 (-93.53%)	25.09 (-93.09 %)	46.15 (-88.68%)	33.44 (-89.91%)	17.27 (-95.66%)	146.46 (-58.47%)
70%	20.84 (-95.04%)	19.45 (-94.65%)	33.91 (-91.68 %)	27.48 (-91.71%)	13.26 (-96.67%)	118.34 (-66.44%)
UCL	4	4	6	10	5	4
h	0.3	0.3	0.7	0.5	0.6	0.1
$\mu_0 = 3,\ \alpha_0 = 0.4$						
δ_μ	$\phi_0 = 0,\ r_0 = 6$	$\phi_0 = 0.4,\ r_0 = 6$	$\phi_0 = 0.7,\ r_0 = 6$	$\phi_0 = 0.8,\ r_0 = 0$	$\phi_0 = 0.8,\ r_0 = 3$	$\phi_0 = 0.8,\ r_0 = 7$
0	409.77	374.47	364.76	378.44	358.64	329.5
5%	309.13 (-24.56%)	260.01 (-30.57%)	254.88 (-30.12%)	272.64 (-27.96%)	222.01 (-38.1%)	294.24 (-10.7%)
10%	238.02 (-41.91%)	185.98 (-50.34%)	182.56 (-49.95%)	203.73 (-46.17%)	147.01 (-59.01%)	260.4 (-20.97%)
20%	148.82 (-63.68%)	103.04 (-72.48%)	101.2 (-72.26%)	124.44 (-67.12%)	76.08 (-78.79%)	198.65 (-39.71%)
30%	98.9 (-75.86%)	62.51 (-83.31%)	61.92 (-83.02%)	83.5 (-77.94%)	46.55 (-87.02%)	147.25 (-55.31%)
40%	69.13 (-83.13 %)	40.87 (-89.09%)	41.32 (-88.67%)	60.15 (-84.11%)	32.02 (-91.07%)	107.67 (-67.32%)
50%	50.45 (-87.69%)	28.42 (-92.41%)	29.61 (-91.88%)	45.77 (-87.91%)	23.9 (-93.34%)	78.94 (-76.04%)
60%	38.19 (-90.68%)	20.8 (-94.45%)	22.46 (-93.84%)	36.37 (-90.39%)	18.88 (-94.74%)	58.79 (-82.16%)
70%	29.83 (-92.72%)	15.85 (-95.77%)	17.8 (-95.12%)	29.94 (-92.09%)	15.56 (-95.66%)	44.83 (-86.39%)
UCL	4	6	5	12	5	5
h	0.1	0.4	0.2	0.4	0.2	0.1
$\mu_0 = 4,\ \alpha_0 = 0.5$						
δ_μ	$\phi_0 = 0,\ r_0 = 6$	$\phi_0 = 0.4,\ r_0 = 6$	$\phi_0 = 0.7,\ r_0 = 6$	$\phi_0 = 0.8,\ r_0 = 0$	$\phi_0 = 0.8,\ r_0 = 3$	$\phi_0 = 0.8,\ r_0 = 7$
0	412.82	365.08	313.13	395.42	365.38	422.51
5%	287.95 (-30.25%)	257.39 (-29.5%)	225.75 (-27.91%)	284.66 (-28.01%)	230.07 (-37.03%)	341.89 (-19.08%)
10%	206.39 (-50%)	186.23 (-48.99%)	165.25 (-47.23%)	212.76 (-46.19%)	156.58 (-57.15%)	273.44 (-35.28%)
20%	113.97 (-72.39%)	104.51 (-71.37%)	93.29 (-70.21 %)	130.2 (-67.07%)	86.26 (-76.39%)	170.92 (-59.55%)
30%	68.26 (-83.46%)	63.43 (-82.63%)	56.34 (-82.01%)	87.58 (-77.85%)	55.75 (-84.74%)	106.1 (-74.89%)
40%	43.73 (-89.41%)	41.05 (-88.76%)	36.18 (-88.45%)	63.22 (-84.01%)	40.04 (-89.04%)	67.06 (-84.13%)
50%	29.58 (-92.83%)	27.95 (-92.34%)	24.54 (-92.16%)	48.1 (-87.84%)	30.96 (-91.53%)	43.83 (-89.63%)
60%	20.92 (-94.93%)	19.84 (-94.57%)	17.37 (-94.45%)	38.14 (-90.35%)	25.18 (-93.11%)	29.84 (-92.94%)
70%	15.41 (-96.27%)	14.57 (-96.01%)	12.78 (-95.92%)	31.23 (-92.1%)	21.29 (-94.17%)	21.18 (-94.99%)
UCL	9	10	10	15	6	10
h	0.7	0.9	0.9	0.4	0.1	0.7

‡The dev$^{(\%)}$ is in parenthesis.

Table 8. The performances of ARL and dev$^{(\%)}$ with combined jumps charts‡.

$\mu_0 = 2,\ \alpha_0 = 0.3$						
δ_μ	$\phi_0 = 0,\ r_0 = 6$	$\phi_0 = 0.4,\ r_0 = 6$	$\phi_0 = 0.7,\ r_0 = 6$	$\phi_0 = 0.8,\ r_0 = 0$	$\phi_0 = 0.8,\ r_0 = 3$	$\phi_0 = 0.8,\ r_0 = 7$
0	407.51	405.15	354.58	342.14	449.36	228.71
5%	326.57 (-19.86%)	331.51 (-18.18%)	304.93 (-14%)	237.12 (-30.7%)	297.03 (-33.9%)	216.86 (-5.18%)
10%	264.44 (-35.11%)	273.93 (-32.39%)	259.72 (-26.75%)	169.56 (-50.44%)	203.88 (-54.63%)	205.15 (-10.3%)
20%	178.44 (-56.21%)	192.01 (-52.61%)	184.35 (-48.01%)	93.99 (-72.53%)	105.81 (-76.45%)	181.58 (-20.61%)
30%	124.35 (-69.49%)	138.66 (-65.78%)	128.87 (-63.66%)	57.03 (-83.33%)	60.84 (-86.46%)	158.06 (-30.89%)
40%	89.08 (-78.14%)	102.7 (-74.65%)	90.03 (-74.61%)	37.23 (-89.12%)	37.91 (-91.56%)	134.73 (-41.09%)
50%	65.38 (-83.96%)	77.61 (-80.84%)	63.58 (-82.07%)	25.81 (-92.46%)	25.2 (-94.39%)	111.91 (-51.07%)
60%	48.97 (-87.98%)	59.7 (-85.26%)	45.68 (-87.12%)	18.82 (-94.5%)	17.61 (-96.08%)	90.67 (-60.36%)
70%	37.35 (-90.83%)	46.6 (-88.5%)	33.48 (-90.56%)	14.3 (-95.82%)	12.83 (-97.14%)	71.66 (-68.67%)
UCL	7	8	7	15	7	8
k	5	5	6	13	5	7
$\mu_0 = 3,\ \alpha_0 = 0.4$						
δ_μ	$\phi_0 = 0,\ r_0 = 6$	$\phi_0 = 0.4,\ r_0 = 6$	$\phi_0 = 0.7,\ r_0 = 6$	$\phi_0 = 0.8,\ r_0 = 0$	$\phi_0 = 0.8,\ r_0 = 3$	$\phi_0 = 0.8,\ r_0 = 7$
0	282.41	402.17	375.53	386.36	327.44	493.04
5%	209.47 (-25.83%)	305.44 (-24.05%)	288.73 (-23.11%)	258.84 (-33.01%)	209.94 (-35.88%)	443.22 (-10.1%)
10%	158.45 (-43.89%)	235.21 (-41.51%)	222.73 (-40.69%)	180.28 (-53.34%)	140.95 (-56.95%)	391.92 (-20.51%)
20%	95.37 (-66.23%)	144.84 (-63.99%)	135.14 (-64.01%)	96.16 (-75.11%)	71.18 (-78.26%)	291.72 (-40.83%)
30%	60.88 (-78.44%)	93.22 (-76.82%)	84.85 (-77.41%)	56.97 (-85.25%)	40.52 (-87.63%)	204.94 (-58.43%)
40%	40.73 (-85.58%)	62.4 (-84.48%)	55.29 (-85.28%)	36.62 (-90.52%)	25.24 (-92.29%)	138.71 (-71.87%)
50%	28.31 (-89.98%)	43.25 (-89.25%)	37.38 (-90.05%)	25.11 (-93.5%)	16.84 (-94.86%)	92.65 (-81.21%)
60%	20.29 (-92.82%)	30.86 (-92.33%)	26.14 (-93.04%)	18.13 (-95.31%)	11.83 (-96.39%)	62.27 (-87.37%)
70%	14.92 (-94.72%)	22.57 (-94.39%)	18.81 (-94.99%)	13.67 (-96.46%)	8.68 (-97.35%)	42.57 (-91.37%)
UCL	8	9	9	19	9	10
k	7	6	6	17	7	7
$\mu_0 = 4,\ \alpha_0 = 0.5$						
δ_μ	$\phi_0 = 0,\ r_0 = 6$	$\phi_0 = 0.4,\ r_0 = 6$	$\phi_0 = 0.7,\ r_0 = 6$	$\phi_0 = 0.8,\ r_0 = 0$	$\phi_0 = 0.8,\ r_0 = 3$	$\phi_0 = 0.8,\ r_0 = 7$
0	368.4	367	395.62	379.26	391.36	365.41
5%	264.24 (-28.27%)	290.96 (-20.72%)	309.48 (-21.77%)	246.52 (-35%)	260.59 (-33.41%)	302.26 (-17.28%)
10%	193.72 (-47.42%)	233.11 (-36.48%)	244.45 (-38.21%)	166.94 (-55.98%)	179.63 (-54.1%)	246.39 (-32.57%)
20%	110.35 (-70.05%)	153.71 (-58.12%)	157.09 (-60.29%)	85.09 (-77.56%)	93.11 (-76.21%)	158.44 (-56.64%)
30%	67.21 (-81.76%)	104.33 (-71.57%)	104.53 (-73.58%)	48.66 (-87.17%)	53.15 (-86.42%)	99.81 (-72.69%)
40%	43.26 (-88.26%)	72.52 (-80.24%)	71.73 (-81.87%)	30.48 (-91.96%)	32.78 (-91.62%)	63.25 (-82.69%)
50%	29.06 (-92.11%)	51.47 (-85.98%)	50.46 (-87.25%)	20.55 (-94.58%)	21.54 (-94.5%)	41.03 (-88.77%)
60%	20.23 (-94.51%)	37.26 (-89.85%)	36.3 (-90.82%)	14.71 (-96.12%)	14.88 (-96.2%)	27.43 (-92.49%)
70%	14.45 (-96.08%)	27.44 (-92.52%)	26.61 (-93.27%)	11.07 (-97.08%)	10.72 (-97.26%)	18.93 (-94.82%)
UCL	10	12	13	24	13	11
k	7	6	6	17	7	8

‡The dev$^{(\%)}$ is in parenthesis.

Table 9. The compare results of CUSUM, EWMA and combined jumps charts with ARL and dev$^{(\%)\ddagger}$.

	$\mu_0 = 1,\ \alpha_0 = 0.3$			$\mu_0 = 3,\ \alpha_0 = 0.4$			$\mu_0 = 5,\ \alpha_0 = 0.5$		
	$\phi_0 = 0.3,\ r_0 = 2$			$\phi_0 = 0.3,\ r_0 = 5$			$\phi_0 = 0.3,\ r_0 = 7$		
δ_μ	CUSUM	EWMA	c-Jump	CUSUM	EWMA	c-Jump	CUSUM	EWMA	c-Jump
0	389.34	318.86	806.34	367.78	381.86	411.13	372.19	361.25	406.29
5%	**252.67 (-35.1%)**	261.73 (-17.92%)	646.72 (-19.8%)	**201.31 (-45.26%)**	265.11 (-30.57%)	312.96 (-23.88%)	**189.86 (-48.99%)**	245.06 (-32.16%)	280.31 (-31.01%)
10%	**180.19 (-53.72%)**	217.5 (-31.79%)	525.13 (-34.87%)	**131.51 (-64.24%)**	189.63 (-50.34%)	241.59 (-41.24%)	**120.23 (-67.7%)**	171.5 (-52.53%)	198.48 (-51.15%)
20%	**110.47 (-71.63%)**	155.14 (-51.35%)	357.33 (-55.68%)	**74.98 (-79.61%)**	105.01 (-72.5%)	149.3 (-63.69%)	**67 (-82%)**	91.2 (-74.75%)	106.62 (-73.76%)
30%	**78.5 (-79.84%)**	114.83 (-63.99%)	252.24 (-68.72%)	**51.8 (-85.92%)**	63.66 (-83.33%)	96.33 (-76.57%)	**45.86 (-87.68%)**	53.18 (-85.28%)	61.82 (-84.78%)
40%	**60.59 (-84.44%)**	87.66 (-72.51%)	183.56 (-77.24%)	**39.37 (-89.3%)**	41.58 (-89.11%)	64.64 (-84.28%)	34.67 (-90.68%)	**33.42 (-90.75%)**	38.26 (-90.58%)
50%	**49.24 (-87.35%)**	68.69 (-78.46%)	137.08 (-83%)	31.67 (-91.39%)	**28.89 (-92.43%)**	44.81 (-89.1%)	27.76 (-92.54%)	22.26 (-93.84%)	**24.88 (-93.88%)**
60%	**41.39 (-89.37%)**	55.05 (-82.74%)	104.8 (-87%)	26.43 (-92.81%)	**21.12 (-94.47%)**	32.01 (-92.21%)	23.09 (-93.8%)	15.57 (-95.69%)	**16.84 (-95.86%)**
70%	**35.67 (-90.84%)**	44.99 (-85.89%)	81.7 (-89.87%)	22.63 (-93.85%)	**16.07 (-95.79%)**	23.46 (-94.29%)	19.72 (-94.7%)	11.33 (-96.86%)	**11.72 (-97.12%)**
UCL	24	2	5	46	6	9	67	11	12
w/h/k	1	0.2	4	3	0.4	6	5	0.8	8
	$\phi_0 = 0.5,\ r_0 = 2$			$\phi_0 = 0.5,\ r_0 = 5$			$\phi_0 = 0.5,\ r_0 = 7$		
δ_μ	CUSUM	EWMA	c-Jump	CUSUM	EWMA	c-Jump	CUSUM	EWMA	c-Jump
0	370.59	314.84	313.94	371.36	361.68	370.83	367.53	466.36	350.37
5%	**241.1 (-34.94%)**	247.96 (-21.24%)	246.91 (-21.35%)	**204.04 (-45.06%)**	252.7 (-30.13%)	279.29 (-24.69%)	**189.91 (-48.33%)**	308.62 (-33.82%)	241.65 (-31.03%)
10%	**172.25 (-53.52%)**	198.32 (-37.01%)	197.32 (-37.15%)	**133.57 (-64.03%)**	181.65 (-49.78%)	213.46 (-42.44%)	**121.02 (-67.07%)**	211.33 (-54.69%)	171.19 (-51.14%)
20%	**105.79 (-71.45%)**	132.34 (-57.97%)	131.3 (-58.18%)	**76.32 (-79.45%)**	101.3 (-71.99%)	129.92 (-64.97%)	**67.74 (-81.57%)**	108.42 (-76.75%)	92.19 (-73.69%)
30%	**75.24 (-79.7%)**	92.53 (-70.61%)	91.55 (-70.84%)	**52.78 (-85.79%)**	61.64 (-82.96%)	83 (-77.62%)	**46.46 (-87.36%)**	61.56 (-86.8%)	53.69 (-84.68%)
40%	**58.11 (-84.32%)**	67.3 (-78.62%)	66.25 (-78.9%)	**40.17 (-89.18%)**	40.3 (-88.86%)	55.3 (-85.09%)	35.16 (-90.43%)	**37.93 (-91.87%)**	33.33 (-90.49%)
50%	**47.23 (-87.26%)**	50.52 (-83.95%)	49.56 (-84.21%)	32.33 (-91.29%)	**27.99 (-92.26%)**	38.17 (-89.71%)	28.18 (-92.33%)	**25.02 (-94.64%)**	21.81 (-93.78%)
60%	**39.71 (-89.28%)**	38.97 (-87.62%)	37.99 (-87.9%)	26.99 (-92.73%)	**20.4 (-94.36%)**	27.18 (-92.67%)	23.47 (-93.61%)	**17.4 (-96.27%)**	14.85 (-95.76%)
70%	**34.25 (-90.76%)**	30.81 (-90.21%)	29.8 (-90.51%)	23.15 (-93.77%)	**15.48 (-95.72%)**	19.88 (-94.64%)	20.06 (-94.54%)	**12.65 (-97.29%)**	10.42 (-97.03%)
UCL	23	4	4	47	7	9	68	11	12
w/h/k	1	0.9	4	3	0.5	6	5	0.7	8
	$\phi_0 = 0.8,\ r_0 = 2$			$\phi_0 = 0.8,\ r_0 = 5$			$\phi_0 = 0.8,\ r_0 = 7$		
δ_μ	CUSUM	EWMA	c-Jump	CUSUM	EWMA	c-Jump	CUSUM	EWMA	c-Jump
0	371.58	419.27	599.01	365.92	362.53	260.78	370.1	366.62	362.9
5%	**239.25 (-35.61%)**	325.86 (-22.28%)	452.35 (-24.48%)	**205.43 (-43.86%)**	275.67 (-23.96%)	193.68 (-25.73%)	**196.76 (-46.84%)**	245.81 (-32.95%)	268.35 (-26.05%)
10%	**169.12 (-54.49%)**	251.01 (-40.13%)	335.28 (-44.03%)	**135.42 (-62.99%)**	210.12 (-42.04%)	143.78 (-44.87%)	**126.63 (-65.78%)**	171.2 (-53.3%)	197.98 (-45.45%)
20%	**102.5 (-72.42%)**	149.79 (-64.27%)	185.83 (-68.98%)	**77.63 (-78.78%)**	125.76 (-65.31%)	80.9 (-68.98%)	**71.26 (-80.75%)**	93.12 (-74.6%)	109.45 (-69.84%)
30%	72.45 (-80.5%)	93.03 (-77.81%)	**109.31 (-81.75%)**	**53.72 (-85.32%)**	79.84 (-77.98%)	47.93 (-81.62%)	**48.98 (-86.77%)**	57.81 (-84.23%)	62.93 (-82.66%)
40%	55.78 (-84.99%)	60.99 (-85.45%)	**68.92 (-88.49%)**	**40.9 (-88.82%)**	54.01 (-85.1%)	30.13 (-88.45%)	**37.14 (-89.96%)**	39.74 (-89.16%)	38.06 (-89.51%)
50%	45.29 (-87.81%)	42.2 (-89.93%)	**46.23 (-92.28%)**	32.97 (-90.99%)	38.75 (-89.31%)	**19.88 (-92.38%)**	29.83 (-91.94%)	29.49 (-91.96%)	**24.2 (-93.33%)**
60%	38.08 (-89.75%)	30.59 (-92.7%)	**32.65 (-94.55%)**	27.58 (-92.46%)	29.28 (-91.92%)	**13.75 (-94.73%)**	24.89 (-93.27%)	23.2 (-93.67%)	**16.05 (-95.58%)**
70%	32.85 (-91.16%)	23.09 (-94.49%)	**24.02 (-95.99%)**	23.67 (-93.53%)	23.1 (-93.63%)	**9.87 (-96.22%)**	21.33 (-94.24%)	19.09 (-94.79%)	**11.09 (-96.94%)**
UCL	22	3	4	48	4	8	72	7	13
w/h/k	1	0.7	3	3	0.1	7	5	0.1	7

‡c-JUMP stands for the combined jumps chart.

Table 10. Estimated parameters, AIC and BIC for the first complaints data set.

Model	Estimators of unknown parameters				AIC	BIC
Poisson INAR(1)	$\hat{\lambda} = 2.4234$	$\hat{\alpha} = 0.2983$			426.1256	431.336
ZIPINAR(1)	$\hat{\alpha} = 0.3675$	$\hat{\lambda} = 2.5955$	$\hat{\rho} = 0.1469$		419.9598	427.7753
GINAR(1)	$\hat{p} = 0.2883$	$\hat{\alpha} = 0.4871$			455.6586	460.869
NGINAR(1)	$\hat{\mu} = 3.1849$	$\hat{\alpha} = 0.6926$			441.1347	446.345
NBINAR(1)	$\hat{\theta} = 6.3551$	$\hat{p} = 0.5427$	$\hat{\alpha} = 0.3487$		423.1237	430.9392
NBRCINAR(1)	$\hat{n} = 8$	$\hat{p} = 0.6989$	$\hat{\rho} = 0.3678$		422.4495	430.265
INAR-GIP(1)	$\hat{r} = 7$	$\hat{\phi} = 0.8353$	$\hat{\lambda} = 1.7061$	$\hat{\alpha} = 0.3878$	414.7315	422.547

Table 11. Estimated parameters, AIC and BIC for the second complaints data set.

Model	Estimators of unknown parameters				AIC	BIC
Poisson INAR(1)	$\hat{\lambda} = 1.5137$	$\hat{\alpha} = 0.2955$			368.7535	373.9638
ZIPINAR(1)	$\hat{\alpha} = 0.2984$	$\hat{\lambda} = 1.7604$	$\hat{\rho} = 0.1351$		365.4889	373.3044
GINAR(1)	$\hat{p} = 0.3515$	$\hat{\alpha} = 0.2354$			393.1489	398.3593
NGINAR(1)	$\hat{\mu} = 2.1359$	$\hat{\alpha} = 0.6768$			378.134	383.3443
NBINAR(1)	$\hat{\theta} = 5.1522$	$\hat{p} = 0.4178$	$\hat{\alpha} = 0.4061$		364.4134	372.2289
NBRCINAR(1)	$\hat{n} = 5$	$\hat{p} = 0.7005$	$\hat{\rho} = 0.3451$		365.228	373.0435
INAR-GIP(1)	$\hat{r} = 6$	$\hat{\phi} = 0.7525$	$\hat{\lambda} = 1.2659$	$\hat{\alpha} = 0.3012$	363.1095	370.925